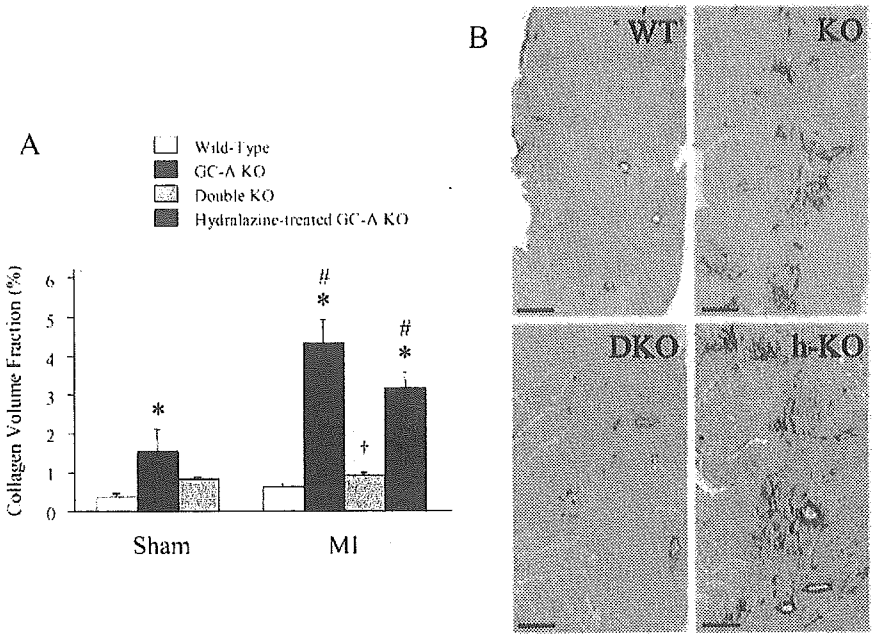

Figure 4. A. Evaluation of collagen volume in sham-operated hearts and noninfarcted regions of infarcted hearts from WT, GC-A KO, DKO, and hydralazine-treated GC-A KO mice 4 weeks after surgery. Values are means±SEM (n=6 to 9); *P<0.05 vs WT mice for each operation; #P<0.05 vs sham-operated KO mice; †P<0.0001 vs KO mice with MI. B, Representative van Gieson–stained sections showing noninfarcted regions in infarcted hearts from WT, GC-A KO (KO), DKO, and hydralazine-treated GC-A KO (h-KO) mice. Images show the interstitial collagen deposition (red staining) 4 weeks after induction of MI. Bars=200 μm.

Discussion

Although plasma ANP and BNP levels are known to be elevated early after MI,[11] their function in that context has been unclear. The present study shows that disrupting GC-A in mice results in a higher incidence of acute heart failure leading to increased early mortality and, later, in exaggerated LV dysfunction and remodeling. Thus, natriuretic peptides appear to exert beneficial effects during the early and late stages after MI.

During the 4-week study period, almost all deaths among both genotypes occurred within the first week after MI and were the result of heart failure or LV rupture. This survival pattern suggests that the rapid worsening of hemodynamics and mechanical stress after MI is, for the most part, compensated by the end of 1 week and stable for ≥3 weeks thereafter. In contrast to our previous study performed using an ischemia-reperfusion model,[13] infarct sizes were similar among the 2 genotypes, which is likely because permanent coronary occlusion changes the entire area at risk into infarction. This enabled us to compare the mortality rates and chronic LV remodeling resulting from similar insults in the 2 groups. Despite similar infarct sizes, the 1-week mortality rate was markedly higher in KO than WT mice. Postmortem findings indicate that the higher 1-week mortality rate in KO mice is attributable to a higher incidence of acute heart failure, which is consistent with the higher levels of cardiac expression of ANP and BNP mRNA observed in KO mice early after MI. Together, these results indicate that KO mice have a diminished capacity to compensate for acute heart failure after MI.

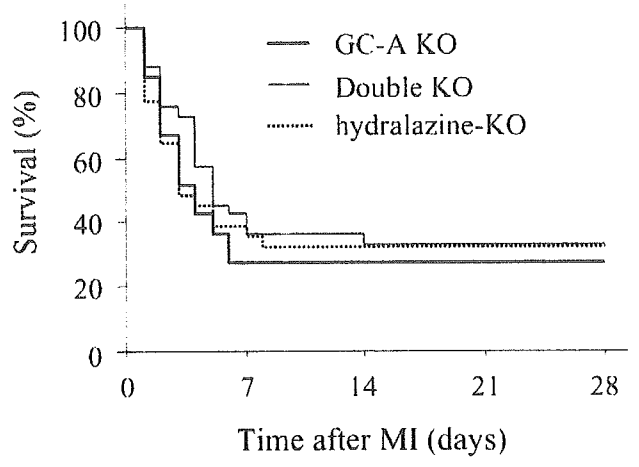

Figure 5. Kaplan–Meier analysis of survival after MI among GC-A KO (n=33), DKO mice (n=33), and hydralazine-treated GC-A KO (hydralazine-KO; n=31) mice. DKO mice and hydralazine-treated GC-A KO showed no significant improvement in 4-week survival over GC-A KO mice.

KO mice excreted less water and sodium than WT mice after MI, despite similar excretion during the early phase after the sham operation. Previous studies have shown that the infusion of 0.9% NaCl containing 4% albumin (isooncotic solution) results in impaired diuretic and natriuretic responses in GC-A KO mice, whereas the infusion of physiological saline (isotonic solution) leads to normal renal responses.[18] Because CHF could cause isooncotic volume expansion, the impaired renal response after MI in GC-A KO mice is consistent with the idea that GC-A plays an important role in diuresis and natriuresis under such pathological conditions as heart failure, although it is not essential under basal conditions.

Natriuretic peptides are known to act as negative regulators of renin-angiotensin-aldosterone system. Indeed, we showed previously that cardiac responsiveness to angiotensin II was significantly enhanced in the absence of GC-A,[16] and a previous study reported that natriuretic peptides reduced gene expression of aldosterone synthase in cultured neonatal rat cardiocytes.[19] In addition, there is clinical and experimental evidence that suppression of RAS activity reduces postinfarction mortality.[1,3,4] Therefore, we hypothesized that the higher mortality in KO mice was associated with greater activation

of RAS resulting from the lack of GC-A–mediated inhibition. To test that hypothesis, we compared postinfarction survival rates in GC-A KO and DKO mice, which lack GC-A and AT1a receptors. However, surprisingly, the 4-week survival rate for DKO mice was no better than that for KO mice, despite their significantly lower basal blood pressures (to a level similar to WT mice), and again most deaths were attributable to acute heart failure. Apparently, the protective role against heart failure played by GC-A early after MI is not mediated by reduction of blood pressure or inhibition of RAS.

GC-A attenuates chronic cardiac remodeling in a pressure-overload model (transverse aortic constriction)[20] and in a chronic hypoxia model.[21] The present study demonstrates that GC-A also attenuates cardiac hypertrophy and fibrosis and impaired LV contractility during the chronic phase after MI. Because previous studies have shown that inhibition of RAS diminishes LV remodeling after MI,[1,4] we were also interested in comparing LV remodeling in DKO and GC-A KO mice. Notably, the patterns of development of myocardial fibrosis and cardiac hypertrophy differed in the 2 genotypes (ie, the augmented fibrotic response was virtually abolished in DKO mice, although there was no attenuation of the enhanced hypertrophic response). Because previous reports have shown that natriuretic peptides exert a direct local antihypertrophic effect in vivo[20,22] and in vitro,[23] it is suggested that a direct action mediated via GC-A expressed on cardiac myocytes may be important after MI. We also evaluated the fibrotic response in hydralazine-treated GC-A KO mice, for which blood pressures were similar to those of DKO mice. However, hydralazine did not significantly affect the fibrotic response in KO mice, indicating the antifibrotic effect of GC-A is mediated mainly through inhibition of RAS, including aldosterone, not through reduction of blood pressure.

A recent clinical trial demonstrated that intravenous infusion of nesiritide (synthetic human BNP) improves the hemodynamic function and clinical status of patients with decompensated CHF.[10] Although patients with recent MIs were excluded from that trial, the present study suggests that infusion of BNP could also have beneficial effects in patients with heart failure early after MI. In addition, a study of 60 Japanese patients with anterior MI showed that infusion of carperitide (recombinant ANP) suppressed LV remodeling evaluated 1 month after MI better than nitroglycerin did.[24] Certainly, the lack of an oral form makes the use of natriuretic peptides somewhat impractical for long-term treatment; nevertheless, therapeutic strategies aimed at increasing levels of endogenous natriuretic peptides might be beneficial for patients after MI and deserve further investigation.

Functional deletion of the 5′-flanking region of the GC-A gene reduces transcriptional activity and is associated with essential hypertension and LV hypertrophy.[25] This means that individuals with congenital or acquired GC-A deficiencies would likely be at higher risk of death and exaggerated LV remodeling after MI. Perhaps genotyping the GC-A locus would be a useful approach to identifying these patients, thereby enabling early preventative measures to be taken.

Perspectives

Activation of GC-A by endogenous natriuretic peptides after MI prevents acute heart failure and attenuates chronic LV remodeling. Although these beneficial effects are mediated partly through inhibition of RAS activity, RAS-independent protective actions of GC-A are also suggested. The results of this study are suggestive of the potential for using exogenous ANP or BNP to improve short- and long-term outcomes among MI patients.

Acknowledgments

This work was supported by research grants from the Japanese Ministry of Education, Science, and Culture; the Japanese Ministry of Health and Welfare; the Japanese Society for the Promotion of Science Research for the Future program; and the KANAE Foundation for Life and Socio-Medical Science. GC-A KO mice were originally generated at the University of Texas, Southwestern Medical Center in Dallas and the Howard Hughes Medical Institute. We thank Kana Okamura and Komaki Okazaki for their excellent secretarial work and Mikako Inoue for her technical help.

References

1. Gruppo Italiano per lo Studio della Sopravvivenza nell'infarto Miocardico. GISSI-3: effects of lisinopril and transdermal glyceryl trinitrate singly and together on 6-week mortality and ventricular function after myocardial infarction. *Lancet.* 1994;343:1115–1122.
2. Dargie HJ. Effect of carvedilol on outcome after myocardial infarction in patients with left-ventricular dysfunction the CAPRICORN randomized trial. *Lancet.* 2001;357:1385–1390.
3. Pfeffer MA, McMurray JJV, Velazguez EJ, Rouleau Jl, Kober L, Maggioni AP, Solomon SD, Swedberg K, Werf FV, White H, Leimberger JD, Henis M, Edwards S, Zelenkofske S, Sellers MA, Califf RM; Valsartan in Acute Myocardial Infarction Trial Investigators. Valsartan, captopril, or both in myocardial infarction complicated by heart failure, left ventricular dysfunction, or both. *N Engl J Med.* 2003;349:1893–1906.
4. Harada K, Sugaya T, Murakami K, Yazaki Y, Komuro I. Angiotensin II type 1A receptor knockout mice display less left ventricular remodeling and improved survival after myocardial infarction. *Circulation.* 1999;100:2093–2099.
5. Nakao K, Ogawa Y, Suga S, Imura H. Molecular biology and biochemistry of the natriuretic peptide system. II: Natriuretic peptide receptors. *J Hypertens.* 1992;10:1111–1114.
6. Yoshimura M, Yasue H, Okumura K, Ogawa H, Jougasaki M, Mukoyama M, Imura H. Different secretion patterns of atrial natriuretic peptide and brain natriuretic peptide in patients with congestive heart failure. *Circulation.* 1993;87:464–469.
7. Maisel AS, Krishnaswamy P, Nowak RM, McCord J, Hollander JE, Duc P, Omland T, Storrow AB, Abraham WT, Wu AH, Clopton P, Steg PG, Westheim A, Knudsen CW, Perez A, Kazanegra R, Herrmann HC, McCullough PA; Breathing Not Properly Multinational Study Investigators. Rapid measurement of B-type natriuretic peptide in the emergency diagnosis of heart failure. *N Engl J Med.* 2002;347:161–167.
8. Stanek B, Frey B, Hulsmann M, Berger R, Sturm B, Strametz-Juranek J, Bergler-Klein J, Moser P, Bojic A, Hartter E, Pacher R. Prognostic evaluation of neurohormonal plasma levels before and during beta-blocker therapy in advanced left ventricular dysfunction. *J Am Coll Cardiol.* 2001;38:436–442.
9. Troughton RW, Frampton CM, Tandle TG, Espiner EA, Nicholls MG, Richards AM. Treatment of heart failure guided by plasma aminoterminal brain natriuretic peptide (N-BNP) concentrations. *Lancet.* 2000;355:1126–1130.
10. Colucci WS, Elkayam U, Horton DP, Abraham WT, Bourge RC, Johnson AD, Wagoner LE, Givertz MM, Liang CS, Neibaur M, Haught WH, LeJemtel TH. Intravenous nesiritide, a natriuretic peptide, in the treatment of decompensated congestive heart failure. *N Engl J Med.* 2000;343:246–253.
11. Morita E, Yasue H, Yoshimura M, Ogawa H, Jougasaki M, Matsumura M, Mukoyama M, Nakao K. Increased plasma levels of brain natriuretic peptide in patients with acute myocardial infarction. *Circulation.* 1993;88:82–91.

12. Omland T, Aakvaag A, Bonarjee VV, Caidahl K, Lie RT, Nilson DW, Sundsfjord JA, Dickstein K. Plasma brain natriuretic peptides as an indicator of left ventricular systolic function and long-term survival after acute myocardial infarction. *Circulation.* 1996;93:1963–1969.
13. Izumi T, Saito Y, Kishimoto I, Harada M, Kuwahara K, Hamanaka I, Takahashi N, Kawakami R, Li Y, Takemura G, Fujiwara H, Garbers DL, Mochizuki S, Nakao K. Blockade of the natriuretic peptide receptor guanylyl cyclase-A inhibits NF-κB activation and alleviates myocardial ischemia/reperfusion injury. *J Clin Invest.* 2001;108:203–213.
14. Lopez MJ, Wong SKF, Kishimoto I, Dubois S, Mach V, Friesen J, Garbers DJ, Beuve A. Salt-resistant hypertension in mice lacking the guanylyl cyclase-A receptor for atrial natriuretic peptide. *Nature.* 1995; 378:65–68.
15. Pfeffer MA, Pfeffer JM, Fishbein MC, Fletcher PJ, Spadaro J, Kloner RA, Braunwald E. Myocardial infarct size and ventricular function in rats. *Circ Res.* 1979;44:503–512.
16. Li Y, Kishimoto I, Saito Y, Harada M, Kuwahara K, Izumi T, Takahashi N, Kawakami R, Tanimoto K, Nakagawa Y, Nakanishi M, Adachi Y, Garbers DL, Fukamizu A, Nakao K. Guanylyl cyclase-A inhibits angiotensin II type 1a receptor-mediated cardiac remodeling, an endogenous protective mechanism in the heart. *Circulation.* 2002;106:1722–1728.
17. Oliver PM, Fox JE, Kim R, Rockman HA, Kim HS, Reddick RL, Pandey KN, Milgram SL, Smithies O, Maeda N. Hypertension, cardiac hypertrophy, and sudden death in mice lacking natriuretic peptide receptor A. *Proc Natl Acad Sci U S A.* 1997;94:14730–14735.
18. Kishimoto I, Dubois SK, Garbers DL. The heart communicates with the kidney exclusively through the guanylyl cyclase-A receptor: acute handling of sodium and water in response to volume expansion. *Proc Natl Acad Sci U S A.* 1996;93:6215–6219.
19. Ito T, Yoshimura M, Nakamura S, Nakayama M, Shimasaki Y, Harada E, Mizuno Y, Yamamuro M, Harada M, Saito Y, Nakao K, Kurihara H, Yasue H, Ogawa H. Inhibitory effect of natriuretic peptides on aldosterone synthase gene expression in cultured neonatal rat cardiocytes. *Circulation.* 2003;107:807–810.
20. Knowles JW, Esposito G, Mao L, Hagaman JR, Fox JE, Smithies O, Rockman HA, Maeda N. Pressure-independent enhancement of cardiac hypertrophy in natriuretic peptide receptor A-deficient mice. *J Clin Invest.* 2001;107:975–984.
21. Klinger JR, Warburton RR, Pietras L, Oliver P, Fox J, Smithies O, Hill NS. Targeted disruption of the gene for natriuretic peptide receptor-A worsens hypoxia-induced cardiac hypertrophy. *Am J Physiol Heart Circ Physiol.* 2002;282:H58–H65.
22. Holtwick R, Eickels MV, Skryabin BV, Baba HA, Bubikat A, Begrow F, Schneider MD, Garbers DL, Kuhn M. Pressure-independent cardiac hypertrophy in mice with cardiomyocyte-restricted inactivation of the atrial natriuretic peptide receptor guanylyl cyclase-A. *J Clin Invest.* 2003;111: 1399–1407.
23. Horio T, Nishikimi T, Yoshihara F, Matsuo H, Takishita S, Kanagawa K. Inhibitory regulation of hypertrophy by endogenous atrial natriuretic peptide in cultured cardiac myocytes. *Hypertension.* 2000;35:19–24.
24. Hayashi M, Tsutamoto T, Wada A, Maeda A, Mabuchi N, Tsutsui T, Horie H, Ohnishi M, Kinoshita M. Intravenous atrial natriuretic peptide prevents left ventricular remodeling in patients with first anterior acute myocardial infarction. *J Am Coll Cardiol.* 2001;37:1820–1826.
25. Nakayama T, Soma M, Takahashi Y, Rehemudula D, Kanmatsuse K, Furuya K. Functional deletion mutation of the 5′-flanking region of type A human natriuretic peptide receptor gene and its association with essential hypertension and left ventricular hypertrophy in the Japanese. *Circ Res.* 2000;86:841–845.

Original Article

Skeletal Muscle AMP-Activated Protein Kinase Phosphorylation Parallels Metabolic Phenotype in Leptin Transgenic Mice Under Dietary Modification

Tomohiro Tanaka,[1] Shuji Hidaka,[1,2] Hiroaki Masuzaki,[1] Shintaro Yasue,[1] Yasuhiko Minokoshi,[3] Ken Ebihara,[1] Hideki Chusho,[1] Yoshihiro Ogawa,[4] Taro Toyoda,[5] Kenji Sato,[6] Fumiko Miyanaga,[1] Muneya Fujimoto,[1] Tsutomu Tomita,[1] Toru Kusakabe,[1] Nozomi Kobayashi,[1] Hideki Tanioka,[1] Tatsuya Hayashi,[7] Kiminori Hosoda,[1] Hironobu Yoshimatsu,[2] Toshiie Sakata,[2] and Kazuwa Nakao[1]

Leptin augments glucose and lipid metabolism independent of its effect on satiety. Administration of leptin in rodents increases skeletal muscle β-oxidation by activating AMP-activated protein kinase (AMPK). We previously reported that, as hyperleptinemic as obese human subjects, transgenic skinny mice overexpressing leptin in liver (LepTg) exhibit enhanced insulin sensitivity and lipid clearance. To assess skeletal muscle AMPK activity in leptin-sensitive and -insensitive states, we examined phosphorylation of AMPK and its target, acetyl CoA carboxylase (ACC), in muscles from LepTg under dietary modification. Here we show that phosphorylation of AMPK and ACC are chronically augmented in LepTg soleus muscle, with a concomitant increase in the AMP-to-ATP ratio and a significant decrease in tissue triglyceride content. Despite preexisting hyperleptinemia, high-fat diet (HFD)-fed LepTg develop obesity, insulin-resistance, and hyperlipidemia. In parallel, elevated soleus AMPK and ACC phosphorylation in regular diet–fed LepTg is attenuated, and tissue triglyceride content is increased in those given HFD. Of note, substitution of HFD with regular diet causes a robust recovery of soleus AMPK and ACC phosphorylation in LepTg, with a higher rate of body weight reduction and a regain of insulin sensitivity. In conclusion, soleus AMPK and ACC phosphorylation in LepTg changes in parallel with its insulin sensitivity under dietary modification, suggesting a close association between skeletal muscle AMPK activity and sensitivity to leptin. *Diabetes* 54:2365–2374, 2005

Leptin, an adipocyte-derived hormone, serves as a master regulator of energy homeostasis by suppressing food intake and enhancing glucose and lipid metabolism (1). Metabolic derangements associated with leptin deficiency and lipoatrophic diabetes have been successfully treated with leptin in murine models and human subjects (2–5). However, mechanisms underlying leptin-induced enhancement in glucose and lipid metabolism have not been fully elucidated. Recent studies have implicated skeletal muscle mitochondrial dysfunction and subsequent intramyocellular lipid accumulation in the pathophysiology of insulin resistance (6). Leptin has the potency of decreasing intramyocellular lipid by enhancing mitochondrial fatty acid β-oxidation (7,8). It has recently been reported that skeletal muscle AMP-activated protein kinase (AMPK), a cellular fuel gauge (9), is critically involved in the process (10).

On the other hand, a growing body of evidence has suggested the presence of insensitivity to leptin in prevalent forms of human obesity and rodent models of diet-induced obesity (DIO) (11). Mechanisms whereby leptin loses its effect under such conditions still remain to be elucidated. To the best of our knowledge, there has been no report to date addressing skeletal muscle AMPK activity under leptin-insensitive states in vivo.

We previously generated transgenic skinny mice overexpressing leptin in liver (LepTg) with elevated plasma leptin concentrations comparable with those of obese human subjects (12). LepTg lack almost all white adipose tissue depots throughout the body but exhibit enhanced glucose and lipid metabolism, providing a unique experimental model to investigate the mechanisms of leptin's metabolic action (4,12–15). Notably, unlike obese hyperleptinemic humans or rodents with DIO, sustained hyperleptinemia in LepTg remains metabolically active. LepTg

From the [1]Department of Medicine and Clinical Science, Kyoto University Graduate School of Medicine, Kyoto, Japan; the [2]Department of Internal Medicine, School of Medicine, Oita University, Oita, Japan; the [3]Department of Developmental Physiology, National Institute for Physiological Sciences, Okazaki, Japan; the [4]Department of Molecular Medicine and Metabolism, Medical Research Institute, Tokyo Medical and Dental University, Tokyo, Japan; the [5]Division of Food Science and Biotechnology, Kyoto University Graduate School of Agriculture, Kyoto, Japan; the [6]Department of Food Sciences and Nutritional Health, Kyoto Prefectural University, Kyoto, Japan; and the [7]Department of Human Coexistence, Kyoto University Graduate School of Human and Environmental Studies, Kyoto, Japan.

Address correspondence and reprint requests to Hiroaki Masuzaki, MD, PhD, Department of Medicine and Clinical Science, Kyoto University Graduate School of Medicine, 54 Shogoin-Kawaharacho, Sakyo-ku, Kyoto 606-8507, Japan. E-mail: hiroaki@kuhp.kyoto-u.ac.jp.

Received for publication 4 January 2005 and accepted in revised form 9 May 2005.

T.T. and S.H. contributed equally to this study.

ACC, acetyl CoA carboxylase; AMPK, AMP-activated protein kinase; DIO, diet-induced obesity; EDL, extensor digitorum longus; FFA, free fatty acid; GTT, glucose tolerance test; HFD, high-fat diet; ITT, insulin tolerance test; SCD-1, stearoyl CoA desaturase-1; UCP-1, uncoupling protein-1.

show increased insulin sensitivity with augmented liver and skeletal muscle insulin receptor signaling (12) and increased whole-body lipid clearance during lipid loading tests (16). These data led us to hypothesize that skeletal muscle AMPK is chronically activated in LepTg.

In the present study, we tested whether augmented insulin sensitivity and lowered plasma lipid levels in LepTg is accompanied by an activation of leptin–skeletal muscle AMPK axis. As long as LepTg are maintained on regular diet, phosphorylation of AMPK and its target, acetyl CoA carboxylase (ACC), is chronically augmented in soleus muscle, a representative oxidative red muscle. Augmented phosphorylation of AMPK and ACC under regular diet is attenuated when LepTg loses its lean, insulin-sensitive phenotype under high-fat diet (HFD). After diet substitution from HFD to regular, LepTg exhibit a higher rate of body weight loss and become more insulin sensitive than nontransgenic littermates (non-Tg), suggesting a rapid recovery of sensitivity to leptin. Early in the process of weight loss, AMPK and ACC phosphorylation are robustly increased in LepTg but not in non-Tg. Our data demonstrate that skeletal muscle AMPK and ACC phosphorylation are in close association with metabolic phenotype in LepTg and shed light upon the physiologic and pathophysiologic roles of the leptin–skeletal muscle AMPK axis.

RESEARCH DESIGN AND METHODS

The generation of transgenic mice has been reported previously (12). Six- to eight-week-old male mice heterozygous for the transgene and non-Tg on C57BL/6N background were used for the experiments. Animals were maintained on regular diet (F-2, 3.73 kcal/g, 11.6% kcal fat, source: soybean; Funahashi Farm, Chiba, Japan) and on a 14-h light/10-h dark cycle at 23°C. Mice were fed HFD or regular diet for 4 or 15 weeks. In another experiment, LepTg and non-Tg maintained on HFD were subjected to diet substitution from HFD to regular. HFD (D12493, 5.24 kcal/g, 60% kcal fat, source: soybean/lard) was purchased from Research Diets (New Brunswick, NJ). Throughout the experiments, animals were allowed free access to food and water. Chloral hydrate (1.6 μg/g i.p.; Nacalai Tesque, Kyoto, Japan) was used for anesthesia. All animal experiments were undertaken in accordance with the guideline for animal experiments of Kyoto University and were approved by the Animal Research Committee, Graduate School of Medicine, Kyoto University.

Metabolic parameters and locomotive activity measurements. Body weight/food intake were recorded daily. Dual-energy X-ray absorptiometry scan (DCS-600EX-III; Aloka, Japan) was undertaken using PHA-601R (Aloka) as a phantom. Vo_2 was measured using a two-chamber Oxymax (MK5000; Muromachi kikai, Tokyo, Japan), an open-circuit indirect calorimetry. Plasma levels for glucose (Tidex; Sankyo, Tokyo, Japan), insulin (ELISA kit; Morinaga, Yokohama, Japan), triglycerides (Triglyceride-E test; Wako, Osaka, Japan), free fatty acids (FFAs) (NEFA-C test; Wako), leptin (mouse leptin radioimmunoassay kit; Linco, St. Charles, MO), and adiponectin (enzyme-linked immunosorbent assay kit; Otsuka, Tokyo, Japan) were measured. For the glucose tolerance test (GTT), mice were fasted for 8 h and were given 1.5 g/kg glucose i.p. (Otsuka). For the insulin tolerance test (ITT), mice were fasted for 3 h and given 1.25 units/kg human regular insulin i.p. (Novo Nordisk, Bagsvaerd, Denmark). Spontaneous locomotion was measured by tracing the distance traveled using infrared camera and Ethovision version 1.9 (Noldus Information Technology). Mice were placed in a dark actometer for a 15-min recording session from 1900 to 2300. Mean values from 3 consecutive days were used.

Muscle triglyceride and adenine nucleotide content measurements. Triglyceride content was measured as previously described (16) using isopropylalcohol/heptane for homogenization. For nucleotides, muscle samples were homogenized in 0.2 mol/l $HClO_4$ (3:80 wt/vol) in an ethanol-dry ice bath, and the supernatant was used for the assay (17). Briefly, the supernatant was neutralized, centrifuged, filtered (0.45-μm Cosmonice filter W; Nacalai Tesque), and then analyzed by high-performance liquid chromatography (DX300; Dionex, Sunnyvale, CA) equipped with an SPD-10Ai detector (Shimadzu, Kyoto, Japan) and Shodex Asahipack GS-320HQ (Showa Denko, Tokyo, Japan) equilibrated with 200 mmol/l sodium phosphate buffer (pH 3.0) at 1 ml/min and monitored at 254 nm.

TABLE 1
Metabolic parameters in leptin transgenic mice under regular diet

	Non-Tg	LepTg
Leptin (ng/ml)	7.6 ± 1.0	39.4 ± 4.2*
Body weight (g)	24.9 ± 1.1	21.7 ± 0.6†
Energy intake (kcal/day)	12.5 ± 0.3	11.6 ± 0.6
Vo_2 (ml · kg$^{-0.75}$ · h^{-1})	1,257 ± 39	1,576 ± 29†
Glucose (mg/dl)	117 ± 7	114 ± 7
Insulin (ng/ml)	1.01 ± 0.09	0.43 ± 0.08†
Triglycerides (mg/dl)	131 ± 5	88 ± 14†
FFAs (mEq/l)	1.82 ± 0.10	1.43 ± 0.08†
Adiponectin (μg/ml)	20.8 ± 1.5	19.7 ± 0.4
Locomotion (m/h)	137 ± 7	177 ± 10†

Data are means ± SE. Six-week-old male mice fed regular diet for 4 more weeks. Body weight and plasma levels for leptin, glucose, insulin, triglycerides, free fatty acids, and adiponectin are from the end of 4 weeks. Blood was obtained ad libitum during 0900–1200. Energy intake is a mean daily caloric intake during 4 weeks. Vo_2 was measured during the 1st week of the period. $n = 10$ for leptin and adiponectin, $n = 7$ for other parameters. *$P < 0.01$, †$P < 0.05$ vs. non-Tg.

Western and Northern blot analyses. Muscle samples were homogenized as previously described (17). Ten milligrams of protein per lane were run on 10% SDS-polyacrylamide gel for AMPK and on 4–10% NuPAGE Bis-Tris gel (Invitrogen, Carlsbad, CA) for ACC and transferred to polyvinylidine fluoride (Perkin Elmer, Boston, MA). Thr172-phosphorylated AMPKα and Ser79-phosphorylated ACC were detected using phospho-specific antibodies. The antibodies are as follows: anti–phospho-Thr172 AMPKα and anti-AMPKα from Cell Signaling Technology (Willmingon, MA) and anti–phospho-Ser79 ACC and anti-ACC from Upstate Biotech (Charlottesville, VA). ECL Plus (Amersham) and an LAS-1000 image analyzer (Fujifilm) were used for the detection, and quantification was by MultiGauge version 2.0 software (Fujifilm). For Northern blotting, liver and brown adipose total RNA was extracted using Trizol reagent (Invitrogen). Northern blot analysis was performed using standard protocol (12). Membranes were hybridized with radiolabeled cDNA probe spanning the coding regions of mouse stearoyl CoA desaturase-1 (SCD-1) or uncoupling protein-1 (UCP-1).

Statistical analyses. Data are means ± SE unless otherwise indicated. Comparison between or among animal groups was undertaken by Student's t test or repeated-measures ANOVA, where applicable, and completed by Fisher's probable least significant difference test.

RESULTS

AMPK and ACC phosphorylation is augmented chronically in soleus muscle from LepTg. Metabolic parameters in LepTg are summarized in Table 1. Along with hyperleptinemia, LepTg exhibit lower plasma insulin, triglyceride, and FFA levels with lower body weight and higher oxygen consumption compared with non-Tg (Table 1). Thr172 phosphorylated; thus, activated AMPKα was significantly increased (150 ± 4% of non-Tg; $P < 0.05$ vs. non-Tg; $n = 7$) in LepTg soleus muscle compared with that from non-Tg (Fig. 1*A*). Concomitantly, Ser79-phosphorylated ACC, an established target of AMPK, was also increased (268 ± 9% of non-Tg; $P < 0.01$ vs. non-Tg; $n = 7$) (Fig. 1*B*). Soleus muscle AMPKα and ACCβ protein levels in LepTg were not significantly different from those in non-Tg (Fig. 1*C* and *D*). In extensor digitorum longus (EDL) muscles, no difference in phosphorylation or protein levels of AMPKα or ACCβ was noted between the genotypes (Fig. 1).

Triglyceride was more abundant in soleus than in EDL muscle (Fig. 1*E*), as previously described (18). In parallel

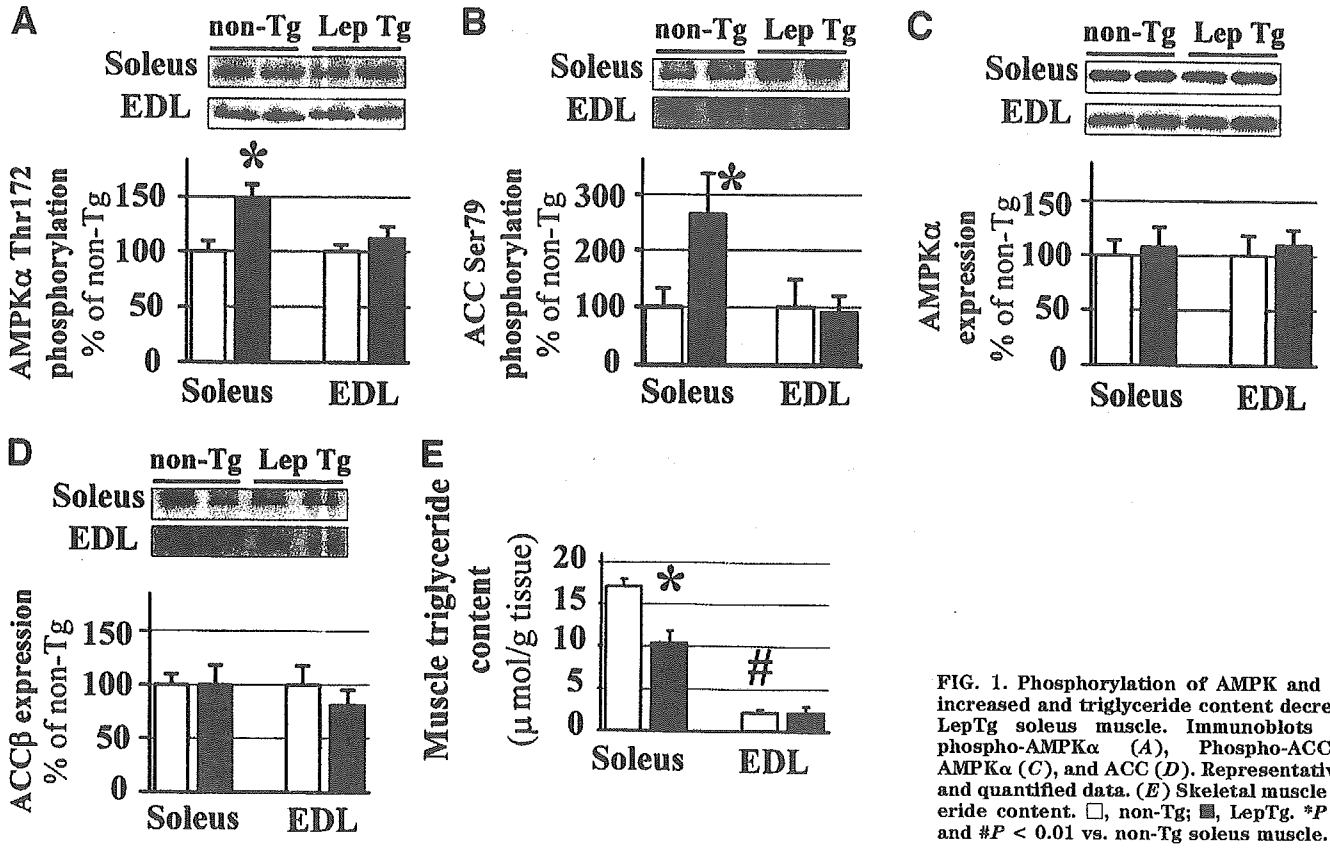

FIG. 1. Phosphorylation of AMPK and ACC is increased and triglyceride content decreased in LepTg soleus muscle. Immunoblots against phospho-AMPKα (*A*), Phospho-ACC (*B*), AMPKα (*C*), and ACC (*D*). Representative blots and quantified data. (*E*) Skeletal muscle triglyceride content. □, non-Tg; ■, LepTg. *$P < 0.05$ and #$P < 0.01$ vs. non-Tg soleus muscle. $n = 7$.

with increased phospho-AMPK and phospho-ACC levels, LepTg soleus muscle contained significantly less triglyceride than non-Tg (61.2 ± 5.9% of non-Tg; $P < 0.05$ vs. non-Tg; $n = 7$) (Fig. 1*E*). In EDL muscle, where phospho-AMPK and phospho-ACC levels were not altered in LepTg, triglyceride levels did not differ between the genotypes.

Apart from leptin, exercise (muscle contraction) and adiponectin are known activators of skeletal muscle AMPK (19–22). Plasma adiponectin levels in LepTg were comparable with those in non-Tg (Table 1). LepTg showed enhanced spontaneous locomotion (Table 1). Although AMPK activity elevated by exercise returns to basal level within an hour after exercise cessation (23), endurance training in humans is associated with upregulated AMPK phosphorylation and activity (24). A possible role of physical activity in enhanced AMPK phosphorylation in LepTg still awaits further investigation.

Increased AMPK and ACC phosphorylation in LepTg soleus muscle is accompanied by increased AMP-to-ATP ratio. AMPK is activated through multiple pathways, including its phosphorylation at Thr172 in its regulatory α-subunit by upstream AMPK kinase (9). AMPK is also allosterically activated by an increase in cellular AMP-to-ATP ratio. Furthermore, the increase in AMP-to-ATP ratio predisposes AMPK for Thr172 phosphorylation and prevents dephosphorylation (9). To unravel the mechanisms underlying chronic increase in AMPK and ACC phosphorylation in LepTg soleus muscle, adenine nucleotide levels were measured. A significant increase in the AMP-to-ATP ratio was observed in LepTg soleus muscle with increased AMP and decreased ATP levels (Table 2). In EDL muscle, the AMP-to-ATP ratio was not altered in transgenics. The increase in the AMP-to-ATP ratio may partly explain the increased AMPK and ACC phosphorylation in LepTg soleus muscle.

LepTg develop obesity, glucose intolerance, insulin resistance, and hyperlipidemia under HFD. When LepTg is genetically crossed with obese/diabetic A^y mice and lipoatrophic A-ZIP/F-1 mice, transgenic overexpression of leptin improves glucose metabolism and insulin sensitivity in these mice (4,13). In this study, we examined whether HFD-induced metabolic derangements are also

TABLE 2
Skeletal muscle adenine nucleotide contents in LepTg mice

	non-Tg		LepTg	
	Soleus	EDL	Soleus	EDL
ATP (nmol/mg muscle)	9.35 ± 0.13	9.49 ± 0.42	8.19 ± 0.19*	10.18 ± 0.52
ADP (nmol/mg muscle)	6.39 ± 0.17	5.67 ± 0.20	6.61 ± 0.19	5.94 ± 0.28
AMP (nmol/mg muscle)	0.24 ± 0.03	0.36 ± 0.02	0.34 ± 0.01†	0.33 ± 0.01
AMP-to-ATP ratio ($\times 10^3$)	25.69 ± 6.30	38.51 ± 7.07	41.86 ± 3.92*	32.28 ± 5.41

Data are means ± SE. Muscles are excised unilaterally from 8- to 10-week-old male mice. Muscles from three mice were pooled in one tube and nucleotide levels measured. $n = \sim 4$–5 pooled samples. *$P < 0.01$, †$P < 0.05$ vs. non-Tg.

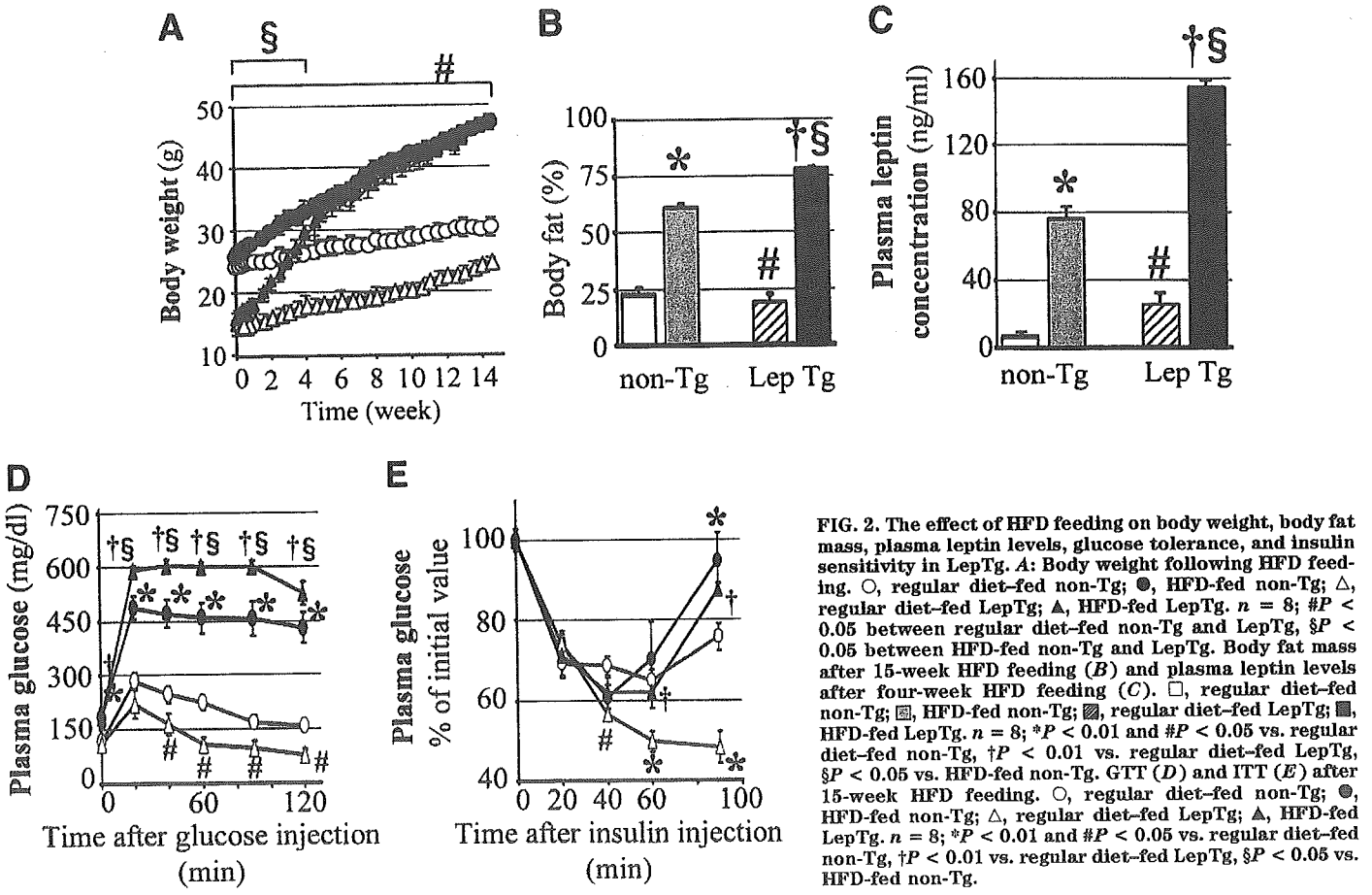

FIG. 2. The effect of HFD feeding on body weight, body fat mass, plasma leptin levels, glucose tolerance, and insulin sensitivity in LepTg. *A*: Body weight following HFD feeding. ○, regular diet–fed non-Tg; ●, HFD-fed non-Tg; △, regular diet–fed LepTg; ▲, HFD-fed LepTg. n = 8; #P < 0.05 between regular diet–fed non-Tg and LepTg, §P < 0.05 between HFD-fed non-Tg and LepTg. Body fat mass after 15-week HFD feeding (*B*) and plasma leptin levels after four-week HFD feeding (*C*). □, regular diet–fed non-Tg; ▨, HFD-fed non-Tg; ▨, regular diet–fed LepTg; ■, HFD-fed LepTg. n = 8; *P < 0.01 and #P < 0.05 vs. regular diet–fed non-Tg, †P < 0.01 vs. regular diet–fed LepTg, §P < 0.05 vs. HFD-fed non-Tg. GTT (*D*) and ITT (*E*) after 15-week HFD feeding. ○, regular diet–fed non-Tg; ●, HFD-fed non-Tg; △, regular diet–fed LepTg; ▲, HFD-fed LepTg. n = 8; *P < 0.01 and #P < 0.05 vs. regular diet–fed non-Tg, †P < 0.01 vs. regular diet–fed LepTg, §P < 0.05 vs. HFD-fed non-Tg.

ameliorated in LepTg. Body weight and body fat mass measured by dual-energy X-ray absorptiometry were significantly lower in LepTg than in non-Tg under regular diet (Fig. 2*A* and *B*). However, after starting on an HFD, both LepTg and non-Tg gained weight. HFD-induced weight gain was more pronounced in LepTg, and the weight of LepTg was comparable with that of non-Tg after 4 weeks of HFD feeding (Fig. 2*A*). Body fat mass after 15 weeks of HFD feeding was even higher in LepTg than in non-Tg (Fig. 2*B*). During the weight gain, both LepTg and non-Tg exhibited an increase in plasma leptin concentration, but the level was significantly higher in LepTg, even under HFD (Fig. 2*C*). In parallel with the loss of a lean phenotype, HFD-fed LepTg lost metabolic advantage and demonstrated an aggravation of glucose tolerance and insulin sensitivity in GTTs and ITTs (Fig. 2*D* and *E*). Under HFD, there was no difference in oxygen consumption or plasma insulin, triglyceride, and FFA levels between the genotypes (Table 3). The development of obesity and the impairment of glucose and lipid metabolism in HFD-fed LepTg indicates that transgenic overexpression of leptin cannot prevent HFD-induced metabolic derangements.

TABLE 3
Metabolic parameters in leptin transgenic mice under HFD

	non-Tg	LepTg
Body weight (g)	32.9 ± 0.7	30.0 ± 0.6
Energy intake (kcal/day)	15.5 ± 0.9	15.5 ± 0.2
Vo_2 (ml · kg$^{-0.75}$ · h^{-1})	1,537 ± 8	1,576 ± 44
Glucose (mg/dl)	145 ± 4	140 ± 10
Insulin (ng/ml)	3.98 ± 0.40	3.07 ± 0.42
Triglycerides (mg/dl)	144 ± 17	143 ± 13
FFAs (mEq/l)	2.11 ± 0.13	2.17 ± 0.16

Data are means ± SE. Six-week-old male mice were fed HFD for 4 weeks. Body weight and plasma levels for glucose, insulin, triglycerides, and free fatty acids are from the end of 4 weeks. Blood was obtained ad libitum during 0900–1200. Energy intake is a mean daily caloric intake during 4 weeks. Vo_2 was measured during the 2nd week of the period. n = 8.

Increased AMPK and ACC phosphorylation and triglyceride reduction in LepTg soleus muscle are abrogated under HFD. We next examined whether augmented AMPK and ACC phosphorylation in LepTg soleus muscle is affected by HFD. HFD feeding for 4 weeks per se did not change phospho-Thr172 AMPKα and phospho-Ser79 ACC levels in non-Tg (Fig. 3*A* and *B*). However, increased phospho-AMPK and phospho-ACC levels in soleus muscle from regular diet–fed LepTg were attenuated under HFD (Fig. 3*A* and *B*). HFD feeding did not affect soleus AMPKα nor ACCβ protein level in both genotypes (Fig. 3*C* and *D*). In EDL muscles, phospho-AMPK, phospho-ACC, AMPKα, and ACCβ levels were unaltered by HFD in both genotypes (data not shown). To test whether attenuated AMPK and ACC phosphorylation under HFD is accompanied by any change in AMP-to-ATP ratio, we measured adenine nucleotide levels in soleus muscle from LepTg fed HFD for 4 weeks (n = ~4–6 pooled samples, 3 muscles per sample). HFD per se led to a 68 ± 16% decrease in AMP and a 26 ± 4% decrease in ADP level in wild-type mice. ATP level was not significantly altered by HFD (12 ± 12% increase), while AMP-to-ATP ratio in

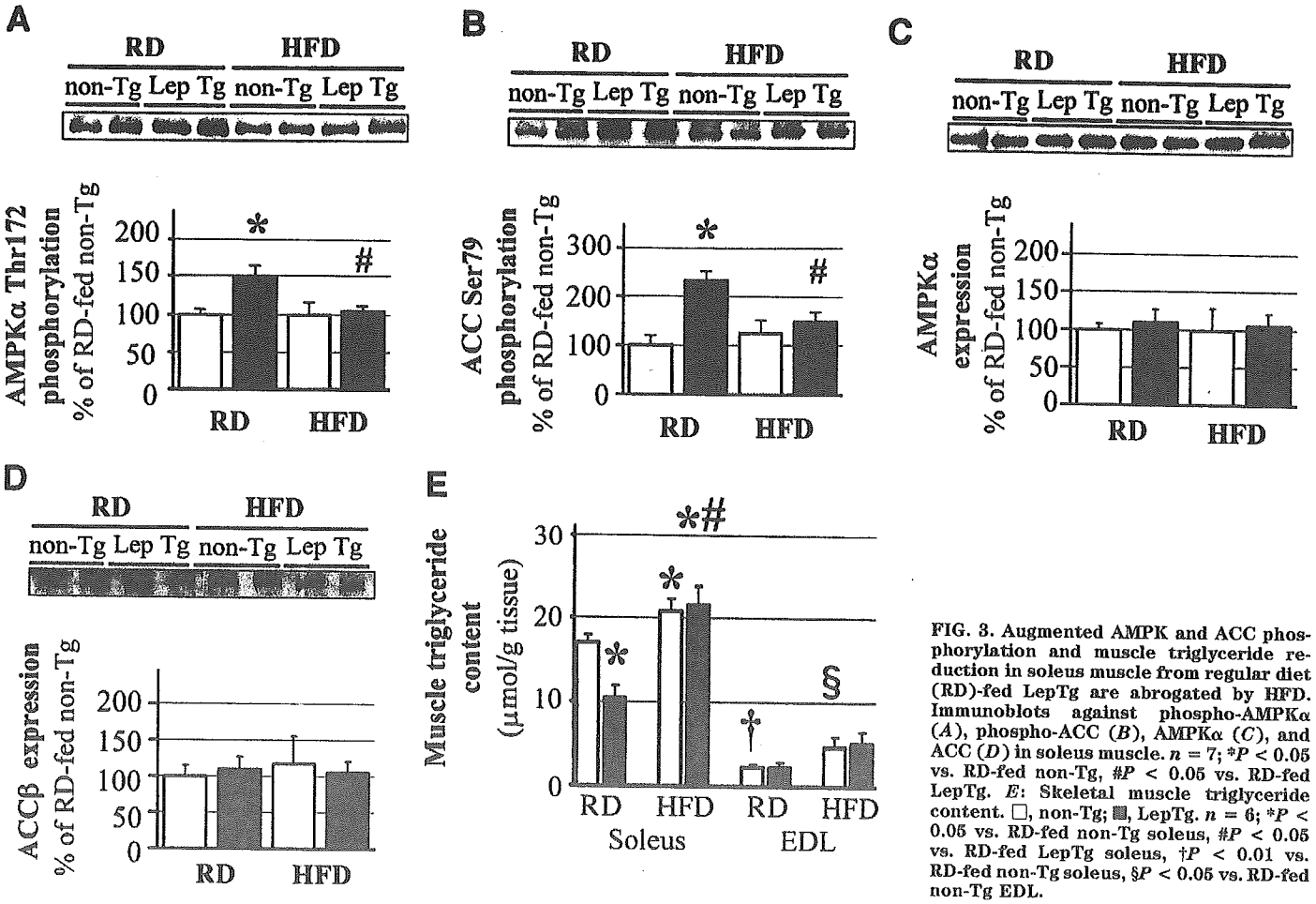

FIG. 3. Augmented AMPK and ACC phosphorylation and muscle triglyceride reduction in soleus muscle from regular diet (RD)-fed LepTg are abrogated by HFD. Immunoblots against phospho-AMPKα (*A*), phospho-ACC (*B*), AMPKα (*C*), and ACC (*D*) in soleus muscle. $n = 7$; *$P < 0.05$ vs. RD-fed non-Tg, #$P < 0.05$ vs. RD-fed LepTg. *E*: Skeletal muscle triglyceride content. □, non-Tg; ■, LepTg. $n = 6$; *$P < 0.05$ vs. RD-fed non-Tg soleus, #$P < 0.05$ vs. RD-fed LepTg soleus, †$P < 0.01$ vs. RD-fed non-Tg soleus, §$P < 0.05$ vs. RD-fed non-Tg EDL.

HFD-fed wild-types tended to be lower than in regular diet–fed wild-types. In HFD-fed LepTg, the AMP level was still significantly higher than in HFD-fed non-Tg (0.43 ± 0.03 vs. 0.16 ± 0.08 nmol/mg muscle, $P < 0.05$). However, there was no significant difference in ATP level or AMP-to-ATP ratio between HFD-fed LepTg and non-Tg. In stark contrast to soleus muscle, AMP, ADP, and ATP levels and AMP-to-ATP ratio in EDL muscle were not altered by HFD, nor was there any difference in these parameters between the genotypes even under HFD. These data raise the possibility that HFD-induced attenuation in soleus muscle AMP-to-ATP ratio may be associated with attenuated AMPK and ACC phosphorylation in HFD-fed LepTg.

HFD feeding led to an increase in tissue triglyceride content both in soleus and EDL muscles (Fig. 3*E*). In contrast to reduced triglyceride content in soleus muscle from regular diet–fed LepTg, the content in HFD-fed LepTg was comparable with that from HFD-fed non-Tg (Fig. 3*E*). In our experimental settings, plasma adiponectin levels increased in response to 4 weeks of HFD feeding, and no difference was observed between HFD-fed LepTg and non-Tg (27.8 ± 3.3 μg/ml in HFD-fed LepTg vs. 23.8 ± 5.2 μg/ml in HFD-fed non-Tg; $n = 6$; not significant).

LepTg lose weight more rapidly after substitution of HFD with regular diet in parallel with a restored AMPK and ACC phosphorylation in soleus muscle. After the 4-week HFD feeding, HFD was substituted with regular diet. Mice were fed ad libitum throughout the study. Diet substitution per se led to a weight loss both in LepTg and non-Tg (Fig. 4*A*). Of note, LepTg exhibited a significantly higher rate of weight loss than non-Tg during the first 7 days (Fig. 4*B*), and LepTg weighed significantly less than non-Tg 14 days after diet substitution (Fig. 4*A*). Plasma leptin concentration returned to pre-HFD levels within 7 days of regular diet feeding in both genotypes, with LepTg maintaining its hyperleptinemia (Fig. 4*C*).

AMPK and ACC phosphorylation in soleus muscle increased only in LepTg and were significantly higher than in similarly treated non-Tg 7 days after diet substitution (Fig. 4*D* and *E*). Of note, restoration in AMPK and ACC phosphorylation preceded the complete resumption of lean phenotype in LepTg (Fig. 4*A*). Neither AMPKα nor ACCβ protein levels were altered by HFD to regular diet substitution (Fig. 4*F* and *G*). Phospho-AMPK, phospho-ACC, AMPKα, and ACCβ levels in EDL muscles remained constant even after diet substitution (data not shown).

GTTs and ITTs were performed following HFD to regular diet substitution. Glucose profiles in GTTs were comparable between the genotypes after diet substitution (Fig. 4*H*). Notably, however, insulin sensitivity was drastically recovered and was enhanced in LepTg compared with similarly treated non-Tg (Fig. 4*I*).

mRNA levels for liver SCD-1 and brown adipose UCP-1 are not associated with metabolic phenotype in LepTg. Leptin-induced downregulation of hepatic SCD-1 expression and activity is reported as an important component of leptin's metabolic action (25–27). SCD-1 is an enzyme that catalyzes the biosynthesis of monounsat-

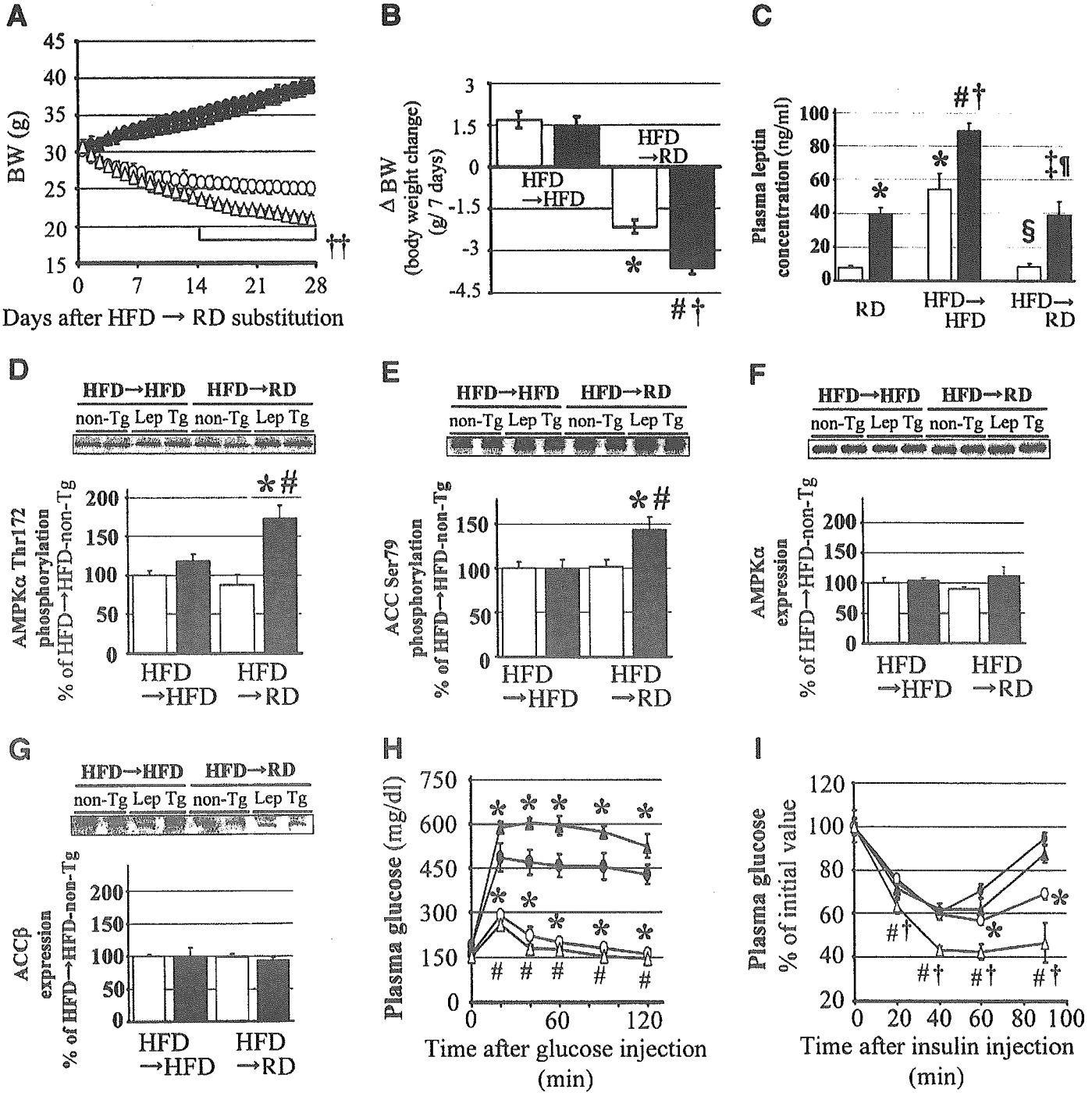

FIG. 4. HFD to regular diet (RD) substitution leads to an accelerated body weight loss and augmented insulin sensitivity in LepTg with a robust recovery of AMPK and ACC phosphorylation. Body weight during the 4 weeks (*A*) and the rate of body weight change during the first 7 days (*B*) following HFD to RD substitution. $n = 10$; *$P < 0.001$ vs. HFD→HFD non-Tg, #$P < 0.001$ vs. HFD→HFD LepTg, †$P < 0.01$ and ††$P < 0.05$ vs. HFD→RD non-Tg. *C*: Plasma leptin levels under RD or after 4-week HFD plus 1-week HFD or RD. $n = 10$; *$P < 0.01$ vs. RD non-Tg, #$P < 0.01$ vs. RD LepTg, †$P < 0.05$ vs. HFD→HFD non-Tg, §$P < 0.01$ vs. HFD→HFD non-Tg, ‡$P < 0.01$ vs. HFD→HFD LepTg, ¶$P < 0.01$ vs. HFD→RD non-Tg. Immunoblots against phospho-AMPKα (*D*), phospho-ACC (*E*), AMPKα (*F*), and ACC (*G*) in soleus muscle (4-week HFD plus 1-week HFD or RD). $n = 7$; *$P < 0.05$ vs. HFD→HFD LepTg, #$P < 0.05$ vs. HFD→RD non-Tg. □, non-Tg; ■, LepTg. GTT (*H*) and ITT (*I*) after 15-week HFD feeding followed by 4-week RD. ●, HFD→HFD non-Tg; ○, HFD→RD non-Tg; ▲, HFD→HFD LepTg; △, HFD→RD LepTg. $n = 8$; *$P < 0.05$ vs. HFD→HFD non-Tg, #$P < 0.05$ vs. HFD→HFD LepTg, †$P < 0.05$ vs. HFD→RD non-Tg.

urated fatty acids. Unexpectedly, SCD-1 mRNA expression in liver was not different between the genotypes (Fig. 5*A*). SCD-1 expression was markedly suppressed by HFD and was not recovered 7 days after HFD to regular diet substitution. These data are consistent with a report that SCD-1 expression is suppressed by polyunsaturated fatty acids (28). mRNA levels were comparable between the genotypes throughout dietary modification (Fig. 5*B*), suggesting that liver SCD-1 expression is not associated with metabolic phenotype in LepTg.

Acute administration of leptin increases brown adipose UCP-1 expression (29). UCP-1 is a crucial factor for

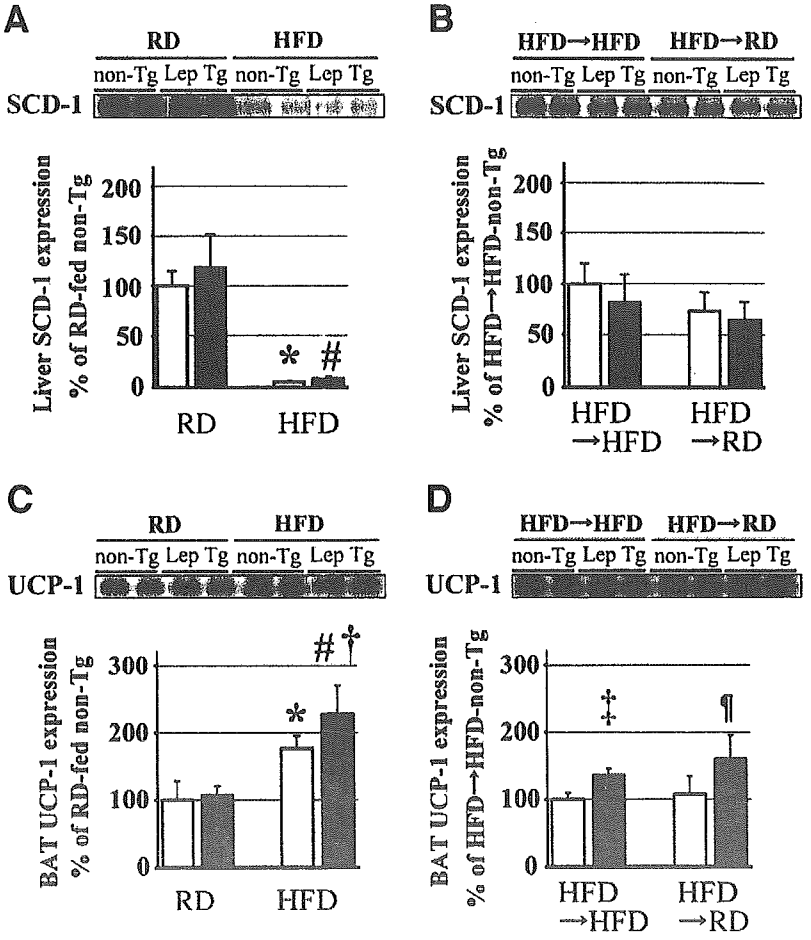

FIG. 5. Northern blot analysis of liver SCD-1 and brown adipose UCP-1 mRNA expression. Liver SCD-1 (*A* and *B*) and brown adipose UCP-1 (*C* and *D*) expression under regular diet (RD), HFD (4 weeks) (*A* and *C*) and 4-week HFD followed by 1-week RD (*B* and *D*). Representative blots and quantified data normalized by 18S rRNA expression. □, non-Tg; ■, LepTg. $n = 5$ (mean ± SD); *$P <$ 0.01 vs. RD-fed non-Tg, #$P <$ 0.01 vs. RD-fed LepTg, †$P <$ 0.05 vs. HFD-fed non-Tg, ‡$P <$ 0.05 vs. HFD→HFD non-Tg, ¶$P <$ 0.01 vs. HFD→RD non-Tg.

nonshivering thermogenesis and energy dissipation in rodents (30) and is suggested as one of the mediators of leptin's insulin-sensitizing action (31). Although LepTg possess a smaller amount of brown adipose tissue than non-Tg (12), brown adipose UCP-1 mRNA expression in LepTg was equivalent to that in non-Tg (Fig. 5*C*). Interscapular brown adipose tissue from LepTg maintains histological characteristics of brown adipose tissue (4). Brown adipose UCP-1 expression was slightly higher in LepTg under HFD and after HFD to regular diet substitution (Fig. 5*D*).

DISCUSSION

Here, we demonstrate that soleus muscle AMPK and ACC phosphorylation is augmented chronically in LepTg. Despite predetermined hyperleptinemia, LepTg is not protected from HFD-induced metabolic derangements, consistent with a previous report that transgenic mice overexpressing leptin in adipocytes are not protected against DIO (32). Noteworthy is that, on an HFD, soleus AMPK and ACC phosphorylation in LepTg is decreased to the level of regular diet–fed or HFD-fed non-Tg. Substitution of HFD with regular diet led to increased AMPK and ACC phosphorylation only in LepTg, with accelerated body weight loss and restored insulin sensitivity. These data suggest that soleus muscle AMPK activity changes in parallel with metabolic action of leptin under nutritional modification. To the best of our knowledge, the present study is the first in addressing the leptin–skeletal muscle AMPK axis under leptin-sensitive and -insensitive states.

AMPK activity is regulated by intracellular energy status as well as upstream AMPK kinase (9,33). Besides allosteric activation of AMPK by AMP, increased AMP-to-ATP ratio predisposes AMPK to be phosphorylated and inhibits its dephosphorylation. In LepTg soleus muscle, AMP-to-ATP ratio was chronically elevated, suggesting a possibility that leptin may chronically regulate skeletal muscle AMPK activity through modulation of cellular energy status in this animal model. Recent studies have suggested LKB1 as a promising candidate for AMPK kinase (34–36). Possible regulation of LKB1 activity by leptin may be an interesting problem to be solved in the future.

In the present study, we used Western blot to examine AMPK phosphorylation. Although increased AMPK phosphorylation cannot be interpreted as an equivalent of AMPK activation as measured by in vitro AMPK assay, data from the AMPK assay performed with immunoprecipitated samples in the presence of abundant AMP and ATP (37) may not necessarily reflect AMPK activity in vivo. The level of AMPKα phosphorylation at Thr172 is closely associated with AMPK activity in many experimental conditions, including leptin-induced AMPK activation in skeletal muscle (10). Our data showing that AMP-to-ATP ratio, AMPK phosphorylation, and ACC phosphorylation were all increased in parallel in LepTg soleus muscle highly suggest enhanced AMPK activity.

Adiponectin activates AMPK in liver and skeletal muscle (21,22). Despite an apparent loss of white adipose tissue in LepTg, there is no significant difference in plasma adiponectin levels between the genotypes. This is in striking

contrast to murine models and human patients with generalized lipodystrophy, where plasma adiponectin levels are extremely low (21,38,39). A lack of difference in plasma adiponectin levels between the genotypes argues against a role of adiponectin in increased AMPK and ACC phosphorylation in LepTg.

Spontaneous locomotive activity is increased in LepTg. Mechanisms whereby hyperleptinemia alters locomotion must await further investigation. A human study (24) using vastus lateralis muscle shows that 3-week supervised endurance training increases AMPK protein levels and basal AMPK activity. Thus, it does not necessarily exclude the possibility that chronically increased locomotion in LepTg may partly contribute to augmented AMPK phosphorylation. However, contraction activates AMPK more readily in white rather than red muscle fibers (40), which marks a sharp contrast to our data indicating that increased AMPK and ACC phosphorylation in LepTg were preferential in soleus muscle. Acute administration of leptin also activates AMPK more readily in red muscles than in white muscles (10). Red muscles have higher rates for oxidation, while white muscles have higher rates for glycolysis (41). The finding that increased AMP-to-ATP ratio, increased AMPK and ACC phosphorylation, and reduced tissue triglyceride content in LepTg all occur preferentially in red muscle further highlights the importance of red muscle as a target for leptin-mediated fuel metabolism. It is interesting to note that muscle fiber-type composition of soleus muscle was not altered in LepTg as assessed by histochemical ATPase activity and also by SDS-PAGE analysis of myosin heavy chain isoforms (T.Ta., T. Ishii, S. Masuda, S. Taguchi, unpublished observation). This suggests that AMPK activation and triglyceride reduction in LepTg soleus muscle is independent of muscle fiber-type switch.

Steinberg et al. (42) have reported that 2-week subcutaneous leptin infusion in rats leads to increased AMPKα2 protein levels along with AMPK phosphorylation in both soleus and white gastrocnemius muscle. They have also found increased ATP level in white gastrocnemius from leptin-treated rats but unaltered ATP and AMP levels in soleus muscle (42). These data are in contrast to ours, showing that AMPKα protein levels were not increased, AMP-to-ATP ratio was increased in LepTg soleus muscle, and AMPK phosphorylation and ATP levels were not changed in EDL muscle. The discrepancy may partly be explained by a difference in species, muscles used, and the extent and duration of hyperleptinemia.

Very recently, a study (43) using human rectus abdominis muscle has demonstrated that in muscle from obese subjects, fatty acid esterification is augmented, while AMPK activity is not downregulated. Consistent with the report, our data clearly show that HFD per se did not change AMPK nor ACC phosphorylation but did increase triglyceride content in non-Tg soleus muscle. In this context, our results may indicate that leptin-induced upregulation of AMPK phosphorylation (but not its basal level) is attenuated in DIO. Treatment of HFD-fed rats and insulin-resistant obese Zucker fatty rats with an AMP mimetic, 5-aminoimidazole-4-carboxamide riboside, enhances AMPK activity and augments liver and muscle insulin sensitivity (40,44), thereby suggesting a therapeutic implication of AMPK activators in leptin-insensitive states.

Under HFD, LepTg exhibit higher rates of body weight gain and higher feed efficiency (milligrams of weight gain per kilocalories of energy intake) than non-Tg (28.2 $\pm$ 1.2 mg/kcal in LepTg vs. 20.8 $\pm$ 1.6 mg/kcal in non-Tg; $P < 0.05$; $n = 8$). Body fat mass is also higher and GTT profile further deteriorated in HFD-fed LepTg than in non-Tg. These data cannot simply be explained by an abrogation of metabolic action of leptin, but would rather suggest a possible role of predetermined hyperleptinemia in exacerbating metabolic derangements under HFD. In accordance with this notion, transgenic mice overexpressing leptin in adipocytes are more prone to HFD-induced obesity (32). The investigators of that study proposed the hypothesis that on an HFD, hyperleptinemia predisposes adipocytes to be hypercellular and hypertrophic (32). Our observation is that skeletal muscle AMPK activity and brown adipose UCP-1 expression in HFD-fed LepTg are comparable with and higher than HFD-fed non-Tg, respectively. Under HFD, no difference was found in energy intake and O_2 consumption between the genotypes as well. The possible role of predetermined hyperleptinemia as a precipitating factor of DIO must await further investigation.

We have previously shown that hyperleptinemia can accelerate the recovery from diabetes in A^{y} mice during caloric restriction, suggesting the potential usefulness of leptin in combination with a caloric restriction for the treatment of obesity-associated diabetes (13). To examine whether hyperleptinemia can augment recovery from HFD-induced obesity and insulin resistance, HFD was substituted with regular diet. After HFD to regular diet substitution, the rate of body weight loss and amelioration in insulin sensitivity were more pronounced in LepTg than in non-Tg. Notably, skeletal muscle AMPK and ACC phosphorylation was increased only in LepTg, suggesting a close association between AMPK activation and insulin sensitivity. Increased AMPK and ACC phosphorylation was observed before LepTg fully regained the lean phenotype. Although LepTg ate less than non-Tg after HFD to regular diet substitution, pair-fed non-Tg weighed significantly heavier than LepTg (T.Ta., unpublished observation). Further studies are necessary to prove a causal role of AMPK in the recovery of insulin sensitivity in LepTg following HFD to regular diet substitution.

Suppression of liver SCD-1 by leptin has been suggested to play a beneficial role in leptin-mediated weight loss in *ob/ob* mice and improvement of steatosis in a murine model of lipoatrophic diabetes (25,26). The finding that leptin improves hepatic insulin resistance in lipoatrophic mice at a low dose that does not alter SCD-1 expression suggests the presence of SCD-1–independent mechanisms (26). In the present study, hepatic SCD-1 expression was not different between the genotypes under any dietary condition, demonstrating that chronic hyperleptinemia in LepTg is not associated with suppressed hepatic SCD-1 expression. A possible role of liver AMPK as an effector molecule of leptin's metabolic action has not been fully investigated and must await further studies.

Unexpectedly, brown adipose UCP-1 expression was not altered in LepTg. This is in contrast to data from acute administration of leptin (29). A recent study (45) has

shown that adenoviral overexpression of leptin in rats increases AMPK and ACC phosphorylation and UCP-1 expression in white adipose tissue, transforming white adipocytes into unique fat-burning cells. In LepTg, white adipose tissue has almost completely disappeared (12), and we could not find such cells even microscopically (4,12). Taken together, brown adipose UCP-1 and other adipocyte molecules are less likely to be associated with leptin sensitivity in LepTg under dietary modification.

In summary, we show that soleus muscle AMPK and ACC phosphorylation is chronically augmented in LepTg, in which hyperleptinemia is associated with enhanced glucose and lipid metabolism. Although HFD feeding attenuates AMPK and ACC phosphorylation and deteriorates insulin sensitivity and plasma lipid profile in LepTg, diet substitution from HFD to regular diet leads to a pronounced restoration of AMPK and ACC phosphorylation and results in an accelerated body weight reduction and recovery of insulin sensitivity. We demonstrate that soleus AMPK and ACC phosphorylation closely parallels metabolic phenotype in LepTg under dietary modification, suggesting a potential link between skeletal muscle AMPK and leptin sensitivity.

ACKNOWLEDGMENTS

This work was supported by a Grant-in-Aid for Scientific Research (B2:16390267 and S2:16109007), a Grant-in-Aid for Exploratory Research (16659243), and a Grant-in-Aid for Scientific Research on Priority Areas (15081101) from The Ministry of Education, Culture, Sports, Science and Technology of Japan; a research grant from the Special Coordination Funds for Promoting Science and Technology; a research award from the Japan Foundation for Applied Enzymology; the Tanita Healthy Weight Community Trust; the Daiwa Securities Health Foundation; the ONO Medical Research Foundation; Yamaguchi Endocrine Research Association; The Ichiro Kanehara Foundation; the Yamanouchi Foundation for Research on Metabolic Disorders; the Cell Science Research Foundation; Takeda Medical Research Foundation; The Study Grant for Japan Insulin Study Group; and the Smoking Research Foundation.

We thank Mayumi Nagamoto, Sayuri Shinhara, Madoka Tsuchiya, Rika Sadato, Keiko Shiiya, and Shiho Yoshiura for assistance. We are grateful to Prof. Sadayoshi Taguchi, Shinya Masuda, Dr. Hidenori Iwai, Dr. Masako Nakano, and Dr. Takako Ishii for valuable technical support and advice.

REFERENCES

1. Friedman JM, Halaas JL: Leptin and the regulation of body weight in mammals. *Nature* 395:763–770, 1998
2. Farooqi IS, Jebb SA, Langmack G, Lawrence E, Cheetham CH, Prentice AM, Hughes IA, McCamish MA, O'Rahilly S: Effects of recombinant leptin therapy in a child with congenital leptin deficiency. *N Engl J Med* 341:879–884, 1999
3. Shimomura I, Hammer RE, Ikemoto S, Brown MS, Goldstein JL: Leptin reverses insulin resistance and diabetes mellitus in mice with congenital lipodystrophy. *Nature* 401:73–76, 1999
4. Ebihara K, Ogawa Y, Masuzaki H, Shintani M, Miyanaga F, Aizawa-Abe M, Hayashi T, Hosoda K, Inoue G, Yoshimasa Y, Gavrilova O, Reitman ML, Nakao K: Transgenic overexpression of leptin rescues insulin resistance and diabetes in a mouse model of lipoatrophic diabetes. *Diabetes* 50:1440–1448, 2001
5. Oral EA, Simha V, Ruiz E, Andewelt A, Premkumar A, Snell P, Wagner AJ, DePaoli AM, Reitman ML, Taylor SI, Gorden P, Garg A: Leptin-replacement therapy for lipodystrophy. *N Engl J Med* 346:570–578, 2002
6. Unger RH: Minireview: Weapons of lean body mass destruction: the role of ectopic lipids in the metabolic syndrome. *Endocrinology* 144:5159–5165, 2003
7. Shimabukuro M, Koyama K, Chen G, Wang M-Y, Trieu F, Lee Y, Newgard CB, Unger RH: Direct antidiabetic effect of leptin through triglyceride depletion of tissues. *Proc Natl Acad Sci U S A* 94:4637–4641, 1997
8. Muoio DM, Dohm GL, Fiedorek FT Jr, Tapscott EB, Coleman RA, Dohm GL: Leptin directly alters lipid partitioning in skeletal muscle. *Diabetes* 46: 1360–1363, 1997
9. Hardie DG: Minireview: The AMP-activated protein kinase cascade: the key sensor of cellular energy status. *Endocrinology* 144:5179–5183, 2003
10. Minokoshi Y, Kim YB, Peroni OD, Fryer LG, Muller C, Carling D, Kahn BB: Leptin stimulates fatty-acid oxidation by activating AMP-activated protein kinase. *Nature* 415:339–343, 2002
11. El-Haschimi K, Pierroz DD, Hileman SM, Bjorbaek C, Flier JS: Two defects contribute to hypothalamic leptin resistance in mice with diet-induced obesity. *J Clin Invest* 105:1827–1832, 2000
12. Ogawa Y, Masuzaki H, Hosoda K, Aizawa-Abe M, Suga J, Suda M, Ebihara K, Iwai H, Matsuoka N, Satoh N, Odaka H, Kasuga H, Fujisawa Y, Inoue G, Nishimura H, Yoshimasa Y, Nakao K: Increased glucose metabolism and insulin sensitivity in transgenic skinny mice overexpressing leptin. *Diabetes* 48:1822–1829, 1999
13. Masuzaki H, Ogawa Y, Aizawa-Abe M, Hosoda K, Suga J, Ebihara K, Satoh N, Iwai H, Inoue G, Nishimura H, Yoshimasa Y, Nakao K: Glucose metabolism and insulin sensitivity in transgenic mice overexpressing leptin with lethal yellow agouti mutation: usefulness of leptin for the treatment of obesity-associated diabetes. *Diabetes* 48:1615–1622, 1999
14. Aizawa-Abe M, Ogawa Y, Masuzaki H, Ebihara K, Satoh N, Iwai H, Matsuoka N, Hayashi T, Hosoda K, Inoue G, Yoshimasa Y, Nakao K: Pathophysiological role of leptin in obesity-related hypertension. *J Clin Invest* 105:1243–1252, 2000
15. Miyanaga F, Ogawa Y, Ebihara K, Hidaka S, Tanaka T, Hayashi S, Masuzaki H, Nakao K: Leptin as an adjunct of insulin therapy in insulin-deficient diabetes. *Diabetologia* 46:1329–1337, 2003
16. Matsuoka N, Ogawa Y, Masuzaki H, Ebihara K, Aizawa-Abe M, Satoh N, Ishikawa E, Fujisawa Y, Kosaki A, Yamada K, Kuzuya H, Nakao K: Decreased triglyceride-rich lipoproteins in transgenic skinny mice overexpressing leptin. *Am J Physiol* 280:E334–E339, 2001
17. Toyoda T, Hayashi T, Miyamoto L, Yonemitsu S, Nakano M, Tanaka S, Ebihara K, Masuzaki H, Hosoda K, Inoue G, Otaka A, Sato K, Fushiki T, Nakao K: Possible involvement of the alpha1 isoform of 5′AMP-activated protein kinase in oxidative stress-stimulated glucose transport in skeletal muscle. *Am J Physiol* 287:E166–E173, 2004
18. Fawcett DW: Muscular tissue, heterogeneity of skeletal muscle fibers. In *Bloom & Fawcett: A Textbook of Histology*. 12th ed. New York, Chapman & Hall, 1994, p. 272
19. Winder WW, Hardie DG: Inactivation of acetyl-CoA carboxylase and activation of AMP-activated protein kinase in muscle during exercise. *Am J Physiol* 270:E2996–E2304, 1996
20. Vavvas D, Apazidis A, Saha AK, Gamble J, Patel A, Kemp BE, Witters LA, Ruderman NB: Contraction-induced changes in acetyl-CoA carboxylase and 5′-AMP-activated kinase in skeletal muscle. *J Biol Chem* 272:13255–13261, 1997
21. Yamauchi T, Kamon J, Minokoshi Y, Ito Y, Waki H, Uchida S, Yamashita S, Noda M, Kita S, Ueki K, Eto K, Akanuma Y, Froguel P, Foufelle F, Ferre P, Carling D, Kimura S, Nagai R, Kahn BB, Kadowaki T: Adiponectin stimulates glucose utilization and fatty-acid oxidation by activating AMP-activated protein kinase. *Nat Med* 8:1288–1295, 2002
22. Tomas E, Tsao TS, Saha AK, Murrey HE, Zhang CC, Itani SI, Lodish HF, Ruderman NB: Enhanced muscle fat oxidation and glucose transport by ACRP30 globular domain: acetyl-CoA carboxylase inhibition and AMP-activated protein kinase activation. *Proc Natl Acad Sci U S A* 99:16309–16313, 2002
23. Musi N, Fujii N, Hirshman MF, Ekberg I, Froberg S, Ljungqvist O, Thorell A, Goodyear LJ: AMP-activated protein kinase (AMPK) is activated in muscle of subjects with type 2 diabetes during exercise. *Diabetes* 50:921–927, 2001
24. Frosig C, Jorgensen SB, Hardie DG, Richter EA, Wojtaszewski JF: 5′-AMP-activated protein kinase activity and protein expression are regulated by endurance training in human skeletal muscle. *Am J Physiol* 286:E411–E417, 2004
25. Cohen P, Miyazaki M, Socci ND, Hagge-Greenberg A, Liedtke W, Soukas AA, Sharma R, Hudgins LC, Ntambi JM, Friedman JM: Role for stearoyl-

CoA desaturase-1 in leptin-mediated weight loss. *Science* 297:240–243, 2002
26. Asilmaz E, Cohen P, Miyazaki M, Dobrzyn P, Ueki K, Fayzikhodjaeva G, Soukas AA, Kahn CR, Ntambi JM, Socci ND, Friedman JM: Site and mechanism of leptin action in a rodent form of congenital lipodystrophy. *J Clin Invest* 113:414–424, 2004
27. Ntambi JM, Miyazaki M, Stoehr JP, Lan H, Kendziorski CM, Yandell BS, Song Y, Cohen P, Friedman JM, Attie AD: Loss of stearoyl-CoA desaturase-1 function protects mice against adiposity. *Proc Natl Acad Sci U S A* 99:11482–11486, 2002
28. Kim HJ, Miyazaki M, Ntambi JM: Dietary cholesterol opposes PUFA-mediated repression of the stearoyl-CoA desaturase-1 gene by SREBP-1 independent mechanism. *J Lipid Res* 43:1750–1757, 2002
29. Satoh N, Ogawa Y, Katsuura G, Numata Y, Masuzaki H, Yoshimasa Y, Nakao K: Satiety effect and sympathetic activation of leptin are mediated by hypothalamic melanocortin system. *Neurosci Lett* 249:107–110, 1998
30. Kozak LP, Harper ME: Mitochondrial uncoupling proteins in energy expenditure. *Annu Rev Nutr* 20:339–369, 2000
31. Hidaka S, Yoshimatsu H, Kondou S, Tsuruta Y, Oka K, Noguchi H, Okamoto K, Sakino H, Teshima Y, Okeda T, Sakata T: Chronic central leptin infusion restores hyperglycemia independent of food intake and insulin level in streptozotocin-induced diabetic rats. *FASEB J* 16:509–518, 2002
32. Ogus S, Ke Y, Qiu J, Wang B, Chehab FF: Hyperleptinemia precipitates diet-induced obesity in transgenic mice overexpressing leptin. *Endocrinology* 144:2865–2869, 2003
33. Hawley SA, Davison M, Woods A, Davies SP, Beri RK, Carling D, Hardie DG: Characterization of the AMP-activated protein kinase kinase from rat liver and identification of threonine 172 as the major site at which it phosphorylates AMP-activated protein kinase. *J Biol Chem* 270:27186–27191, 1996
34. Woods A, Johnstone SR, Dickerson K, Leiper FC, Fryer LG, Neumann D, Schlattner U, Wallimann T, Carlson M, Carling D: LKB1 is the upstream kinase in the AMP-activated protein kinase cascade. *Curr Biol* 13:2004–2008, 2003
35. Hawley SA, Boudeau J, Reid JL, Mustard KJ, Udd L, Makela TP, Alessi DR, Hardie DG: Complexes between the LKB1 tumor suppressor, STRAD alpha/beta and MO25 alpha/beta are upstream kinases in the AMP-activated protein kinase cascade. *J Biol* 2:1–16, 2003
36. Sakamoto K, Goransson O, Hardie DG, Alessi DR: Activity of LKB1 and AMPK-related kinases in skeletal muscle: effects of contraction, phenformin and AICAR. *Am J Physiol* 287:E310–E317, 2004
37. Hayashi T, Hirshman MF, Fujii N, Habinowski SA, Witters LA, Goodyear LJ: Metabolic stress and altered glucose transport: activation of AMP-activated protein kinase as a unifying coupling mechanism. *Diabetes* 49:527–531, 2000
38. Colombo C, Cutson JJ, Yamauchi T, Vinson C, Kadowaki T, Gavrilova O, Reitman ML: Transplantation of adipose tissue lacking leptin is unable to reverse the metabolic abnormalities associated with lipoatrophy. *Diabetes* 51:2727–2733, 2002
39. Haque WA, Shimomura I, Matsuzawa Y, Garg A: Serum adiponectin and leptin levels in patients with lipodystrophies. *J Clin Endocrinol Metab* 87:2395, 2002
40. Iglesias MA, Ye JM, Frangioudakis G, Saha AK, Tomas E, Ruderman NB, Cooney GJ, Kraegen EW: AICAR administration causes an apparent enhancement of muscle and liver insulin action in insulin-resistant high-fat–fed rats. *Diabetes* 51:2886–2894, 2002
41. Berchtold MW, Brinkmeier H, Muntener M: Calcium ion in skeletal muscle: its crucial role for muscle function, plasticity, and disease. *Physiol Rev* 80:1215–1265, 2000
42. Steinberg GR, Rush JW, Dyck DJ: AMPK expression and phosphorylation are increased in rodent muscle after chronic leptin treatment. *Am J Physiol* 284:E648–E654, 2003
43. Steinberg GR, Smith AC, Van Denderen BJ, Chen Z, Murthy S, Campbell DJ, Heigenhauser GJ, Dyck DJ, Kemp BE: AMP-activated protein kinase is not down-regulated in human skeletal muscle of obese females. *J Clin Endocrinol Metab* 89:4575–4580, 2004
44. Buhl ES, Jessen N, Pold R, Ledet T, Flyvbjerg A, Pedersen SB, Pedersen O, Schmitz O, Lund S: Chronic treatment with 5-aminoimidazole-4-carboxamide-1-β-D-ribofuranoside increases insulin-stimulated glucose uptake and GLUT4 translocation in rat skeletal muscles in a fiber type–specific manner. *Diabetes* 51:2199–2206, 2002
45. Orci L, Cook WS, Ravazzola M, Wang MY, Park BH, Montesano R, Unger RH: Rapid transformation of white adipocytes into fat-oxidizing machines. *Proc Natl Acad Sci U S A* 101:2058–2063, 2004

Available online at www.sciencedirect.com

SCIENCE DIRECT

European Journal of Pharmacology 508 (2005) 255–265

www.elsevier.com/locate/ejphar

Therapeutic potential of thiazolidinediones in activation of peroxisome proliferator-activated receptor γ for monocyte recruitment and endothelial regeneration

Tokuji Tanaka[1], Yasutomo Fukunaga[1], Hiroshi Itoh*, Kentaro Doi, Jun Yamashita, Tae-Hwa Chun, Mayumi Inoue, Ken Masatsugu, Takatoshi Saito, Naoki Sawada, Satsuki Sakaguchi, Hiroshi Arai, Kazuwa Nakao

Department of Medicine and Clinical Science, Kyoto University Graduate School of Medicine, 54 Shogoin Kawahara-cho, Sakyo-ku, Kyoto 606-8507, Japan

Received 8 July 2004; received in revised form 18 October 2004; accepted 28 October 2004
Available online 30 December 2004

Abstract

Thiazolidinediones, a new class of antidiabetic drugs that increase insulin sensitivity, have been shown to be ligands for peroxisome proliferator-activated receptor γ (PPARγ). Recent studies demonstrating that PPARγ occurs in macrophages have focused attention on its role in macrophage functions. In this study, we investigated the effect of thiazolidinediones on monocyte proliferation and migration in vitro and the mechanisms involved. In addition, we examined the therapeutic potentials of thiazolidinediones for injured atherosclerotic lesions. Troglitazone and pioglitazone, the two thiazolidinediones, as well as 15-deoxy-Δ12,14-prostaglandin J2 inhibited in a dose-dependent manner the serum-induced proliferation of THP-1 (human monocytic leukemia cells) and of U937 (human monoblastic leukemia cells), which permanently express PPARγ. These ligands for PPARγ also significantly inhibited migration of THP-1 induced by monocyte chemoattractant protein-1 (MCP-1). Troglitazone and 15-deoxy-Δ12,14-prostaglandin J2 significantly suppressed the mRNA expression of the MCP family-specific receptor CCR2 (chemokine CCR2 receptor) in THP-1 at the transcriptional level. Furthermore, troglitazone significantly inhibited MCP-1 binding to THP-1. Oral administration of troglitazone to Watanabe heritable hyperlipidemic (WHHL) rabbits after balloon injury suppressed acute recruitment of monocytes/macrophages and accelerated re-endothelialization. These results suggest that thiazolidinediones have therapeutic potential for the treatment of diabetic vascular complications.

Keywords: Thiazolidinedione; PPARγ; MCP-1; CCR2; Macrophage; Insulin resistance

1. Introduction

Recruitment of circulating monocytes and their proliferation and differentiation into macrophages are not only the central events for initiation and progression of atherosclerosis, but have also been recently recognized as crucial pathogenic events in both diabetic micro- and macroangiopathy. Monocyte chemoattractant protein (MCP)-1 is a member of the C-C branch (or β) of the chemokine family and a potent monocyte and lymphocyte chemoattractant, which is expressed abundantly in atherosclerosic lesions (Nelken et al., 1991). MCP-1 initiates signal transduction through binding to the chemokine CCR2 receptor (CCR2) (Charo et al., 1994). In a study of CCR2 knockout mice, markedly fewer macrophages were present in the aorta of CCR2−/−, apoE−/− double knockout mice than in that of apoE−/− mice (Boring et al., 1998). Moreover, an independent study demonstrated that MCP-1−/− mice, when crossed with LDL receptor−/− mice, had smaller lesions and a significant reduction of macrophages in the lesions (Gu et al., 1998). These findings indicate the direct role of MCP-1 and CCR2 in monocyte recruitment and atherosclerosis.

* Corresponding author. Tel.: +81 75 751 3170; fax: +81 75 771 9452.
E-mail address: hiito@kuhp.kyoto-u.ac.jp (H. Itoh).
[1] These two authors contributed equally to this work.

0014-2999/$ - see front matter © 2004 Elsevier B.V. All rights reserved.
doi:10.1016/j.ejphar.2004.10.056

Thiazolidinediones are a new class of antidiabetic agents that increase sensitivity to insulin (Nolan et al., 1994). Insulin resistance has been attracting attention as the common casual factor not only for diabetes mellitus but also for hypertension, hyperlipidemia and obesity, all of which are risk factors for atherosclerosis (DeFronzo and Ferrannini, 1991). Recently, thiazolidinediones have been shown to be the ligands for peroxisome proliferator-activated receptor γ (PPARγ), which is a member of the nuclear receptor superfamily of ligand-activated transcription factors and has been identified as the functional receptor in antidiabetic action of thiazolidinediones (Lehmann et al., 1995).

PPARγ and the retinoid X receptor contain a heterodimer to bind regulatory elements in the promoter region of a number of adipocyte-specific genes and stimulate transcription (Tontonoz et al., 1994). In a previous study, we cloned rat PPARγ and detected down-regulation of PPARγ mRNA by several cytokines (Tanaka et al., 1999). Recent studies have demonstrated that PPARγ is expressed in cells of monocyte/macrophage lineage (Ricote et al., 1998; Tontonoz et al., 1998), and that oxidized low density lipoprotein (oxLDL), which plays a central role in atherogenesis, can regulate PPARγ-dependent gene transcription (Nagy et al., 1998). We recently reported that oxLDL potentiates, through the activation of PPARγ, the expression of vascular endothelial growth factor (VEGF) in human endothelial cells and in monocytes/macrophages (Inoue et al., 2001). Another study demonstrated that the administration of troglitazone, one of the thiazolidinediones, to Watanabe heritable hyperlipidemia (WHHL) rabbits and high fat-fed low density lipoprotein receptor or apo E knockout mice inhibits progression of atherosclerosis (Shiomi et al., 1999; Chen et al., 2001; Collins et al., 2001). All of these studies indicate the significance of PPARγ in monocyte and macrophage functions and atherogenesis.

The objective of the study presented here was to determine the effect of thiazolidinediones on the migration and proliferation of monocytes/macrophages and to investigate the molecular mechanism of the effect of thiazolidinediones on MCP-1-induced monocyte migration, with the focus on the expression of CCR2. Furthermore, we used WHHL atherosclerotic rabbits for an in vivo investigation of the therapeutic potentials of thiazolidinediones for acute monocyte recruitment and infiltration as well as for endothelial regeneration after acute vascular injury.

2. Materials and methods

2.1. Cell culture

THP-1 (human monocytic leukemia cells) and U937 (human monoblastic leukemia cells) were obtained from ATCC and cultured as previously reported (Inoue et al., 2001), with or without the following agents: troglitazone (Sankyo, Tokyo, Japan), pioglitazone (Takeda Chemical Industries, Osaka, Japan), 15-deoxy-Δ12,14-prostaglandin J2 (Sigma, St. Louis, MO), which is one of the natural ligands of PPARγ, or 9-*cis*-retinoic acid (Sigma), which is the ligand of the retinoid X receptor.

2.2. Northern blot analysis

Total cellular RNA was isolated from cultured cells using TRIzol reagents (Gibco BRL, Gaithersburg, MD). Northern blot analysis was performed as described elsewhere (Tanaka et al., 1999). The human PPARγ probe consisted of an 858-base pair fragment of the cDNA corresponding to nucleotides 329–1186 of the human PPARγ1 cDNA. The human CCR2 probe consisted of a 939-base pair fragment of the CCR2 cDNA corresponding to nucleotides 1–939. A human β-actin probe (Wako, Japan) was used to monitor the amount of total RNA in each sample.

2.3. Establishment of U937 cells permanently expressing PPARγ

U937 cells permanently expressing PPARγ were established by using the PPARγ expression vector (pCMX-mPPARγ), which contains a cytomegalovirus enhancer and mouse full-length PPARγ cDNA, as we previously reported and explained in detail (Inoue et al., 2001).

2.4. Chemotaxis assay

The cell migration was evaluated with the modified Boyden chamber technique using a 96-well chemotaxis chamber (Neuroprobe, Cabin John, MD) with 50 μl of cell suspension (2×10^7 cells/ml cells in Roswell Park Memorial Institute medium (RPMI)), as previously reported by us (Sawada et al., 2000).

2.5. Equilibrium binding analysis

The cells were suspended at a density of 2×10^7 cells/ml in 200 μl of binding buffer containing 0.1% bovine serum albumin. The cells were incubated with 0.02 nM ^{125}I-MCP-1 and various amounts of unlabelled ligand for 90 min at 25 °C. All assays were done in triplicate, and binding data were examined with the Ligand Assistance Program (Ligand Pharmaceuticals, Charlotte, NC) or Scatchard analysis.

2.6. Balloon angioplasty and troglitazone administration

Homozygous male WHHL rabbits (10 months old, 3.6±0.1 kg) were used for this study. The rabbits were supplied by Sankyo Pharmaceutical. All animals used in the present study were treated with humane care in compliance with the *Guide for the Care and Use of Laboratory Animals* prepared by the National Academy of Sciences and published by the National Institutes of Health (NIH

publication No. 85-23, revised 1985). Each WHHL rabbit was fully anesthetized with sodium pentobarbital (25 mg/kg body weight). A 4F Fogarty balloon catheter was inserted from the left femoral artery, and after the balloon was inflated with air (0.3 ml in the thoracic region and 0.2 ml in the abdominal region), the intima of the thoracic and abdominal aorta was denuded by three passages of the catheter, as we previously reported (Doi et al., 2001). One group (n=8) received troglitazone at a concentration of 100 mg/kg body weight/day from 2 weeks before the angioplasty until 6 weeks after the balloon treatment and the other group (n=8) was given a control solvent. Two rabbits in the control group died during the catheterization and were dropped from the study.

2.7. Pathological examination, immunohistochemical analysis and evaluation of re-endothelialization

The rabbits were fully anesthetized and then killed 6 weeks after the angioplasty. Thirty minutes before they were killed, the animals received an intravenous injection of 6 mL of 0.5% Evans blue dye delivered via the ear vein to identify the remaining non-endothelialized area, as previously described by us (Doi et al., 2001). The area of the intimal surface that was stained blue after the application of Evans blue dye was considered to represent the portion of the arterial segment that remained endothelium deficient. Computerized planimetry (NIH image ver 1.61) was used for analysis. Next, two segments each from the thoracic aorta and the abdominal aorta were obtained from each rabbit (four sites per rabbit). The segments were fixed in methanol–Carnoy's fixative and processed routinely, embedded in paraffin and sectioned into 5-μm-thick slices. The serial sections from each segment were stained with hematoxylin–eosin or with the anti-smooth muscle actin monoclonal antibody (mAb) (1A4; Deckman) or with anti-rabbit macrophage mAb RAM11 (Dako), as we previously reported (Inoue et al., 1998). The acute recruitment or infiltration of macrophages after the angioplasty was evaluated by counting the number of RAM-11$^+$ macrophages on the surface of the aorta (see Fig. 6).

2.8. Reverse transcription-polymerase chain reaction (RT-PCR) for VEGF

The aorta was frozen in liquid N2 immediately after sacrifice and stored at −80 °C until further study. The frozen aorta was homogenized in cold TRIzol reagent (Invitrogen) and total RNA was extracted according to the manufacturer's instructions. cDNA synthesis was performed with 1 μg of total RNA, oligo(dT)20 and ThermoScript (Invitrogen). Incubation lasted for 40 min at 55 °C. The sense primer for rabbit VEGF was 5′GTGGACATCTT CCAGG AGTA-3′and the antisense primer 5′TCTTTGGTCTGCATTCAC A-3′as described previously (Skorjanc et al., 1998). For rabbit G3PDH, the sense primer was 5′ACCACGGTGCACGCCATCAC-3′ and the antisense primer was 5′TCCACCA CCCTGTTGCTGTA-3′ PCR was performed with 2 μL of cDNA template, 2.5U Platinum Taq DNA Polymerase (Invitrogen) and 0.4 μM of the sense and antisense primers. The annealing temperature was 57 °C for VEGF and 60 °C for G3PDH and the number of cycles was 30 for both. Product detection [226 nucleotides for VEGF and 450 for G3PDH] was performed after electrophoresis on 2% agarose gel using ethidium bromide staining.

2.9. Statistical analysis

All values were expressed as mean±S.E.M. Factorial analysis of variance (ANOVA) followed by the Fischer's protected least significant difference test was used to identify significant differences in multiple comparisons.

3. Results

3.1. Induction of PPARγ expression by PPARγ and retinoid X receptor ligands in monocytes/macrophages

PPARγ mRNA was not detected in U937 whether treated or not with PPARγ and retinoid X receptor ligands. While unstimulated THP-1 expressed PPARγ mRNA at a low level, treatment of THP-1 with PPARγ ligands (10^{-5} mol/l troglitazone, 10^{-5} mol/l pioglitazone, or 10^{-5} mol/l 15-deoxy-Δ12,14-prostaglandin J2) or retinoid X receptor ligand (10^{-7} mol/l 9-*cis*-retinoic acid) resulted in a significant increase of PPARγ expression in THP-1. Stimulation with a combination of troglitazone and 9-*cis*-retinoic acid resulted in further up-regulation of PPARγ mRNA expression (Fig. 1).

3.2. Inhibition of proliferation of THP-1 by PPARγ and retinoid X receptor ligands

Cells (1.0×10^5 cells/ml) were cultured for 5 days in the presence of various doses of one of the thiazolidinediones, 15-deoxy-Δ12,14-prostaglandin J2, 9-*cis*-retinoic acid or combination thereof. When cells were treated with vehicle alone, the number of cells significantly increased 7.2 times after 5 days in culture. Troglitazone, pioglitazone, 15-deoxy-Δ12,14-prostaglandin J2 or 9-*cis*-retinoic acid caused a concentration-dependent suppression of cell growth. With 10^{-5} mol/l troglitazone, pioglitazone, 15-deoxy-Δ12,14-prostaglandin J2 and 10^{-7} mol/l 9-*cis*-retinoic acid alone, cell proliferation was inhibited by 60%, 51%, 56% and 39%, respectively, after 5 days. The simultaneous treatment of cells with both 10^{-5} mol/l troglitazone and 10^{-7} mol/l 9-*cis*-retinoic acid produced a 77% inhibition of cell growth. No effect was observed with troglitazone (10^{-5} mol/l) when used alone or in combination with 9-*cis*-retinoic acid (10^{-7} mol/l) in U937 cells in which PPARγ was not detected.

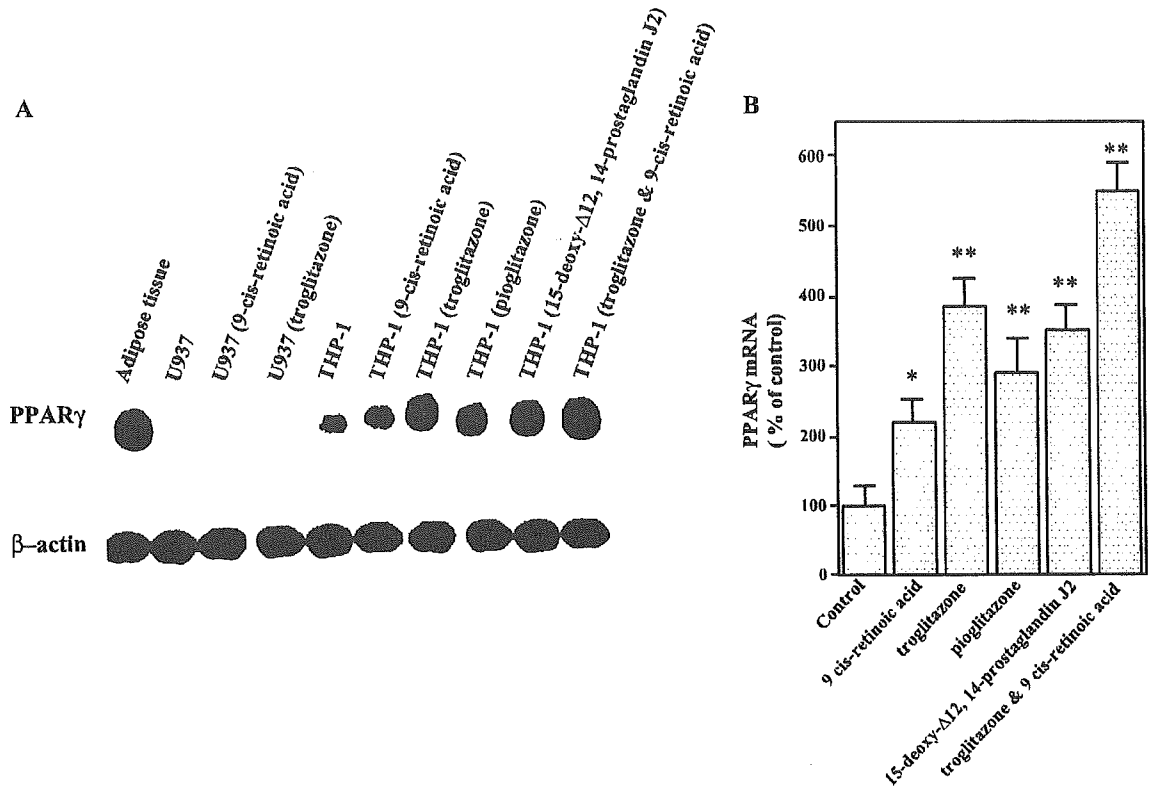

Fig. 1. Induction of PPARγ mRNA expression by PPARγ and retinoid X receptor ligands in monocytes/macrophages. U937 and THP-1 were incubated with 10^{-5} mol/l of troglitazone, pioglitazone, and 15-deoxy-Δ12,14-prostaglandin J2 and with 10^{-7} mol/l of 9-*cis*-retinoic acid for 24 h and their effects on PPARγ mRNA expression were evaluated by Northern blot analysis. (A) Northern blot analysis of PPARγ mRNA in adipose tissue, U937, and THP-1. Twenty micrograms of total RNA per lane were used for the analysis. (B) Quantitative measurements of PPARγ mRNA levels in THP-1. $^{*}P<0.05$ and $^{**}P<0.01$ vs. corresponding controls (n=4).

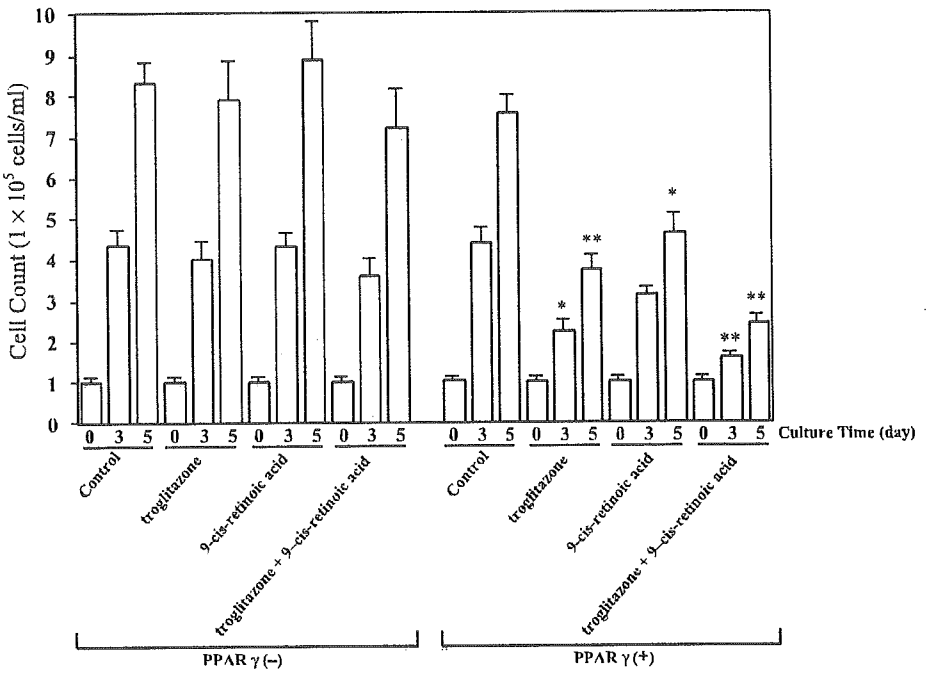

Fig. 2. Inhibition of proliferation of U937 cell expressing PPARγ by troglitazone and 9-*cis*-retinoic acid. Wild-type U937 cells and U937 cells stably transfected with PPARγ expression vector were plated at 1.0×10^5 cells/ml and cultured for 5 days in the presence of 10^{-5} mol/l of troglitazone and 10^{-7} mol/l of 9-*cis*-retinoic acid alone or in combination. Cell numbers were counted after 3 and 5 days. $^{*}P<0.05$ and $^{**}P<0.01$ vs. corresponding controls (n=4).

3.3. Restoration of responsiveness to troglitazone and 9-cis RA in U937 expressing PPARγ

To further characterize the role of PPARγ in monocytes/macrophages proliferation, we utilized the permanent cell line of U937 expressing PPARγ. As shown in Fig. 2, troglitazone or 9-*cis*-retinoic acid treatment of these cell lines resulted in a marked inhibition of cell growth, similar to that of THP-1. With 10^{-5} mol/l of troglitazone alone, cell proliferation was inhibited by 56% after 5 days, and with 10^{-7} mol/l 9-*cis*-retinoic acid alone by 45%. Moreover, treatment of the cells with a combination of 10^{-5} mol/l troglitazone and 10^{-7} mol/l 9-*cis*-retinoic acid resulted in a 71% inhibition of cell growth (Fig. 2).

3.4. Inhibition of MCP-1-induced migration of THP-1 by PPARγ and retinoic X receptor ligands

The chemotactic response of THP-1 to MCP-1, troglitazone, 15-deoxy-Δ12,14-prostaglandin J2 and 9-*cis*-retinoic acid was assessed during a 2-h incubation. The treatment with MCP-1 resulted in a dose-dependent induction in the migration of THP-1 (5 To 50 ng/ml), but THP-1 cells did not show a significant migratory response to troglitazone, 15-deoxy-Δ12,14-prostaglandin J2 or 9-*cis*-retinoic acid. Pretreatment with troglitazone for 24 h significantly inhibited the migration of THP-1 induced by MCP-1 (25 ng/ml), and with 10^{-7} mol/l troglitazone, the migration of THP-1 was inhibited by 44%. Maximal inhibition (66%, $P<0.01$) of THP-1 migration was observed in response to treatment with 10^{-4} mol/l troglitazone (Fig. 3A). Pretreatment with 15-deoxy-Δ12,14-prostaglandin J2 or 9-*cis*-retinoic acid also inhibited the migration of THP-1 under the same conditions (Fig. 3B,C), while troglitazone and 9-*cis*-retinoic acid (10^{-7} mol/l) had an even more profound inhibitory effect on migration (Fig. 3D).

3.5. Regulation of CCR2 mRNA expression by troglitazone, 15-deoxy-Δ12,14-prostaglandin J2 and 9-cis RA In THP-1

We also examined the effect of troglitazone, 15-deoxy-Δ12,14-prostaglandin J2 and 9-*cis*-retinoic acid on CCR2

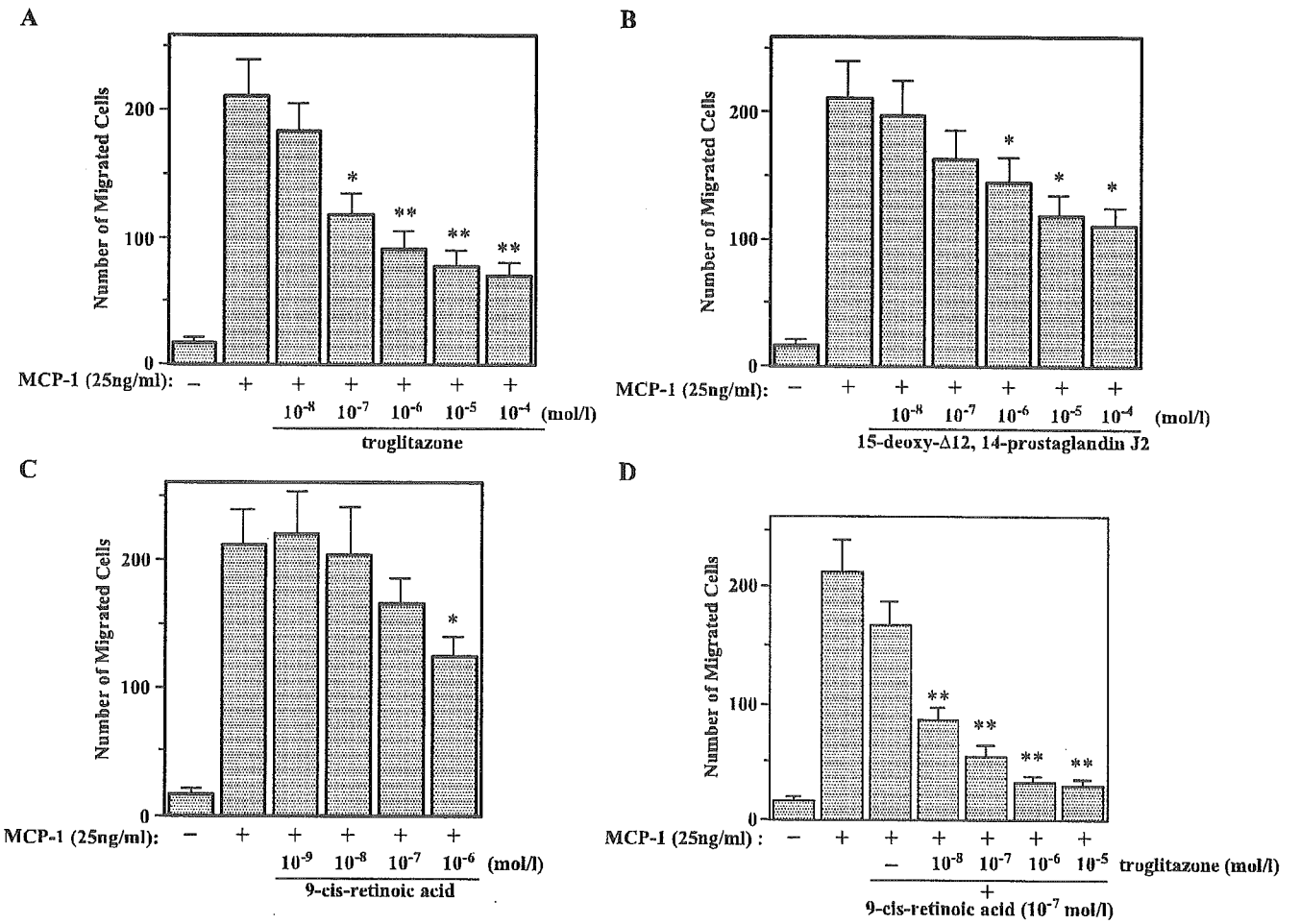

Fig. 3. Inhibition of MCP-1-induced migration of THP-1 by PPARγ and retinoid X receptor ligands. THP-1 were pretreated with different concentrations of troglitazone (A), 15-deoxy-Δ12,14-prostaglandin J2 (B), 9-*cis*-retinoic acid (C) alone or in combination with troglitazone and 9-*cis*-retinoic acid (D) for 24 h at 37 °C. MCP-1 (25 ng/ml) was added to the lower wells as the chemoattractant and 2 h migration assays were performed ($n=6$). *$P<0.05$ and **$P<0.01$ vs. 25 ng/ml of MCP-1 alone.

expression. treatment with 10^{-5} mol/l troglitazone resulted in a time-dependent reduction in the expression of CCR2 mRNA. The inhibitory effect of 10^{-5} mol/l of troglitazone was first observed after a 6-h incubation and persisted for at least a 48-h exposure (Fig. 4A). Treatment with troglitazone (10^{-7} mol/l to 10^{-4} mol/l) suppressed CCR2 mRNA expression in a dose-dependent fashion (Fig. 4B,C). The maximum decrease of 93% occurred in response to 10^{-4} mol/l of troglitazone. Treatment with 15-deoxy-Δ12,14-prostaglandin J2 (10^{-6}–10^{-4} mol/l) and with 9-*cis*-retinoic acid (10^{-7}–10^{-6} mol/l) also suppressed the CCR2 mRNA level in a dose-dependent fashion (Fig. 4B,C).

To determine whether the down-regulation of CCR2 is a transcriptional or post-transcriptional event, we analyzed the effect of troglitazone on the expression of CCR2 mRNA in the presence of actinomycin D (3 μg/ml, Sigma), a transcriptional inhibitor. When treated with actinomycin D, a linear decrease in the level of CCR2 mRNA without the treatment of troglitazone was observed (T1/2; 3 h). With the treatment of troglitazone, the level of CCR2 mRNA also

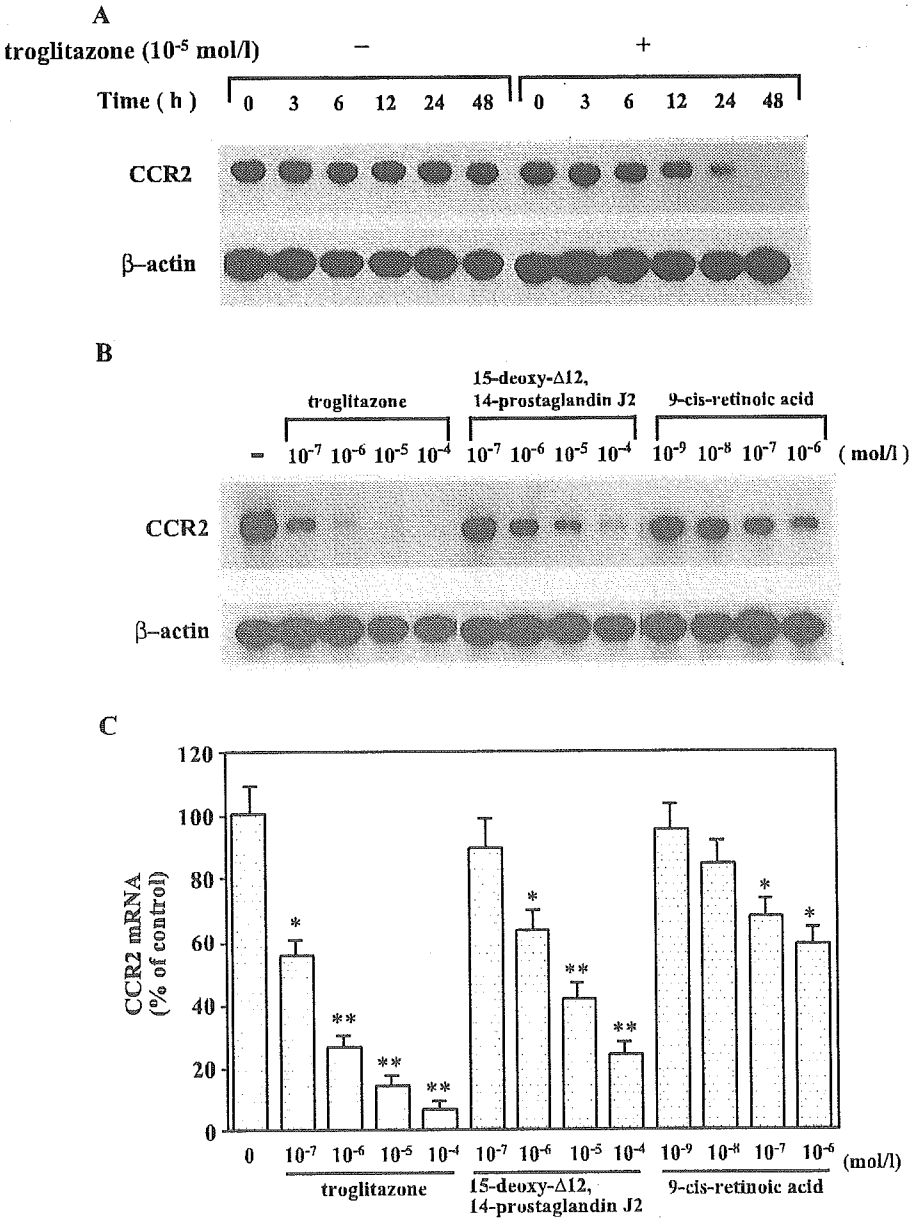

Fig. 4. Regulation of CCR2 mRNA expression by troglitazone, 15-deoxy-Δ12,14-prostaglandin J2 or 9-*cis*-retinoic acid in THP-1. (A) Time-dependent effect of troglitazone on CCR2 mRNA expression. THP-1 cells were incubated with or without 10^{-5} mol/l of troglitazone and harvested after various incubation times for RNA isolation. Twenty micrograms of total RNA per lane was used for the analysis. Similar results were obtained in three independent experiments. (B) Concentration-dependent effect of troglitazone, 15-deoxy-Δ12,14-prostaglandin J2 and 9-*cis*-retinoic acid on CCR2 mRNA expression. THP-1 were incubated with or without various concentrations of troglitazone, 15-deoxy-Δ12,14-prostaglandin J2 and 9-*cis*-retinoic acid harvested 24 h after incubation. Twenty micrograms of total RNA per lane was used for the analysis. (C) Quantitative measurements of CCR2 mRNA levels after administration of troglitazone, 15-deoxy-Δ12,14-prostaglandin J2, or 9-*cis*-retinoic acid. *$P<0.05$ and **$P<0.01$ vs. corresponding controls ($n=4$).

decreased, but at a similar rate to that of the control not treated with troglitazone (Fig. 5A,B).

3.6. Inhibition of MCP-1 binding to THP-1 by troglitazone and 9-cis RA

Under the same experimental condition as described above, we also examined the effects of troglitazone on the binding of MCP-1 to THP-1. THP-1 was pretreated for 24 h with or without 10^{-5} mol/l of troglitazone. As illustrated in Fig. 6A, Scatchard analysis showed that K_d values were similar for the control and troglitazone-treated groups (0.61±0.13 nmol/l for the control and 0.65±0.16 nmol/l for the troglitazone-treated group). In contrast, the troglitazone-treated THP-1 expressed 4.3±0.8 fmol of receptors/10^6 cells, while the control THP-1 expressed 11.7±1.6 fmol/10^6 cells. Thus, troglitazone (10^{-5} mol/l) reduced the number of MCP-1 receptor on the cell surface by 64%. Fig. 6B shows the time course of the effect of troglitazone and 9-*cis*-retinoic acid on the binding of MCP-1 to THP-1. At 10^{-5} mol/l of troglitazone alone, the binding was inhibited by 51% after 12 h and by 66% after 24 h, and the simultaneous treatment of cells with 10^{-5} mol/l troglitazone and 10^{-7} mol/l 9-*cis*-retinoic acid resulted in 85% inhibition.

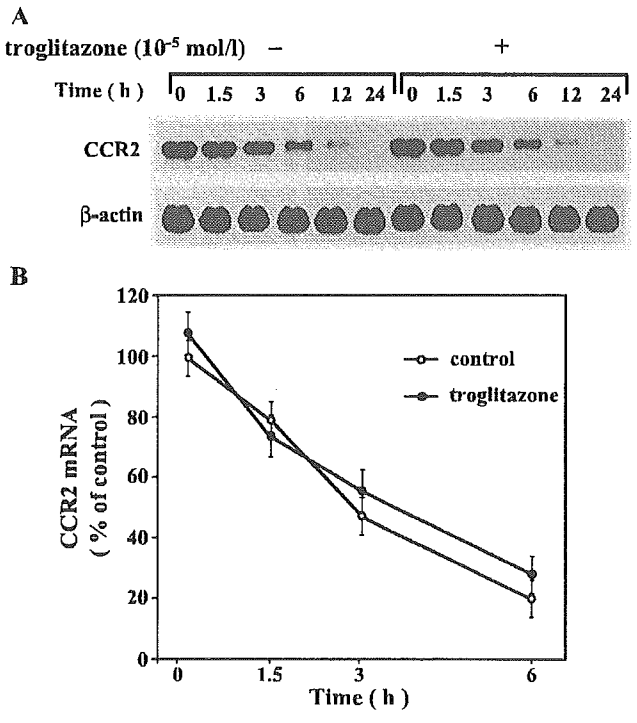

Fig. 5. Effect of troglitazone on the expression of CCR2 mRNA in the presence of actinomycin D. (A) THP-1 were incubated with 3 μg/ml of actinomycin D with or without 10^{-5} mol/l of troglitazone for 24 h and harvested after various incubation times for RNA isolation. Twenty micrograms of total RNA per lane was used for the analysis. (B) Quantitative measurements of CCR2 mRNA levels after treatment with 3 μg/ml of actinomycin D with or without 10^{-5} mol/l of troglitazone (n=3).

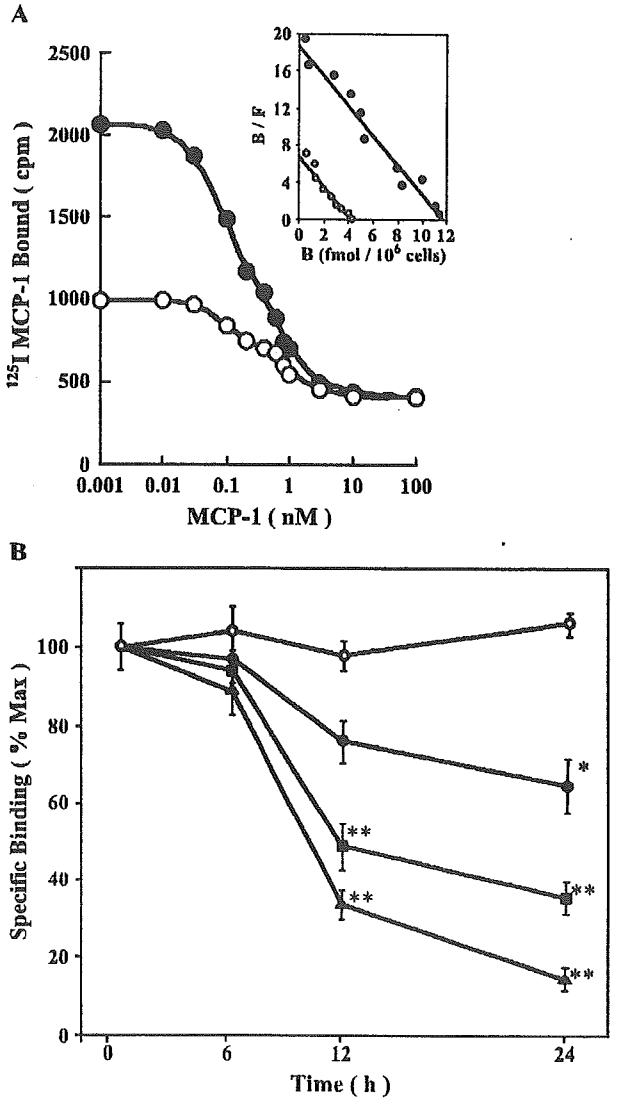

Fig. 6. Inhibition of MCP-1 binding to THP-1 by troglitazone and 9-*cis*-retinoic acid. (A) ^{125}I-labelled MCP-1 binding curve and Scatchard plot analysis. THP-1 were pretreated with (white circles) or without (black circles) 10^{-5} mol/l of troglitazone for 24 h at 37 °C. Insets show Scatchard analysis of the specific binding data. The results are representative of three independent experiments. (B) Time course of troglitazone and 9-*cis*-retinoic acid-induced reduction of MCP-1 binding to THP-1. The cells were incubated for up to 24 h at 37 °C without treatment (white circle) or with 10^{-5} M of troglitazone (black square) or 10^{-7} mol/l of 9-*cis*-retinoic acid (black circle) alone or in combination (black triangle). The binding of ^{125}I-MCP-1 was determined in the presence or absence of 100 nmol/l of unlabeled MCP-1. *P<0.05 and **P<0.01 vs. corresponding controls.

3.7. Suppression by troglitazone of monocyte and macrophage recruitment onto the balloon-injured aorta of WHHL rabbits

At the end of the study, 10-month-old WHHL rabbits belonging to the control group exhibited severe atherosclerotic lesions in thoracic aortae (61±11% of the total surface area) and patchy lesions in abdominal aortae (37±9%). Treatment with troglitazone for a total of 8 weeks did not